Western Alps and the Alpine Foreland

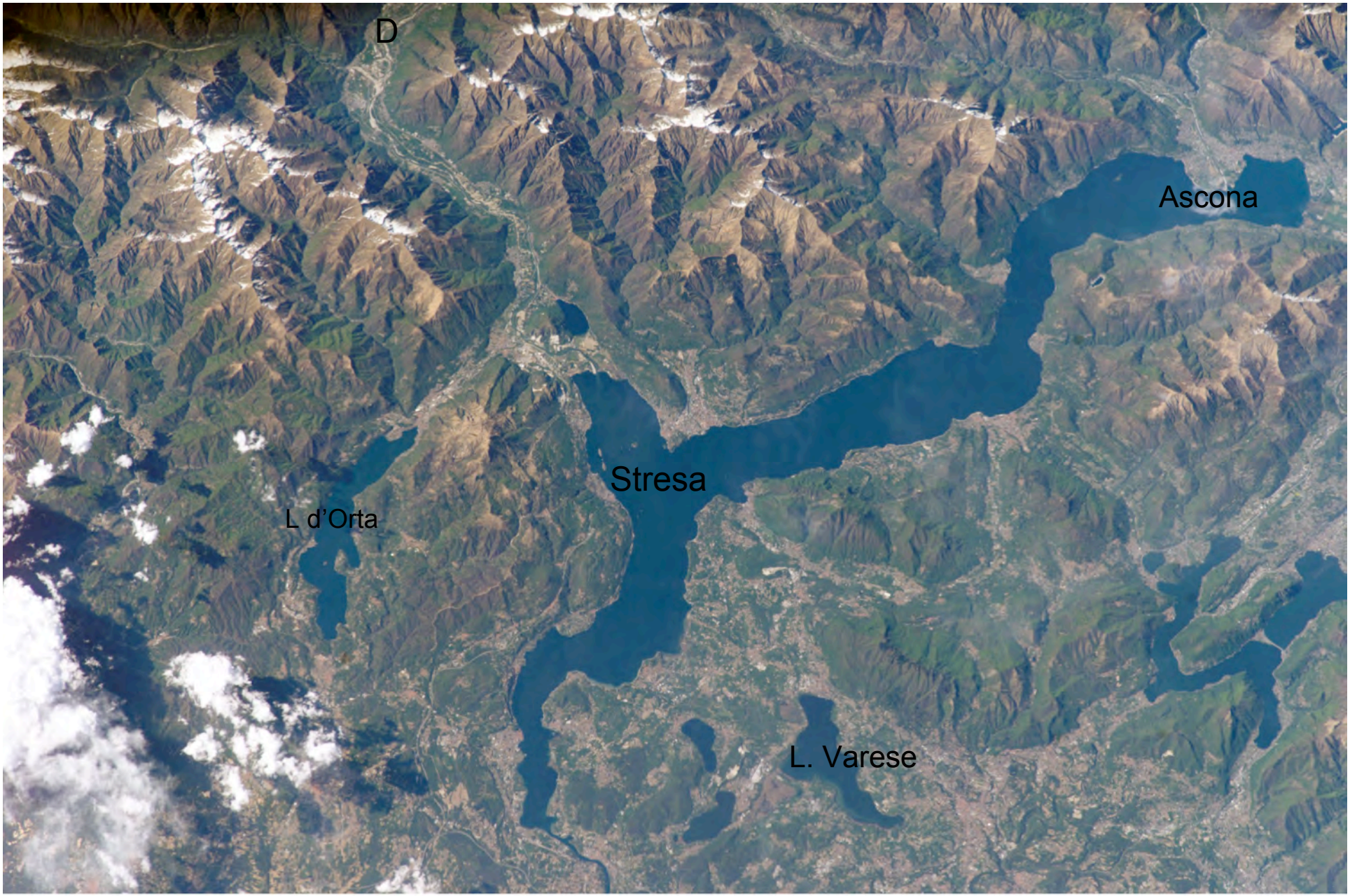

ISS004E10699

Italian Alps: Lago Maggiore

http://eol.jsc.nasa.gov/

Isola Bella, Lago Maggiore view to north

ISS004E11806

Alps: Lake Leman, Rhone Valley, Monte Bianco http://eol.jsc.nasa.gov/

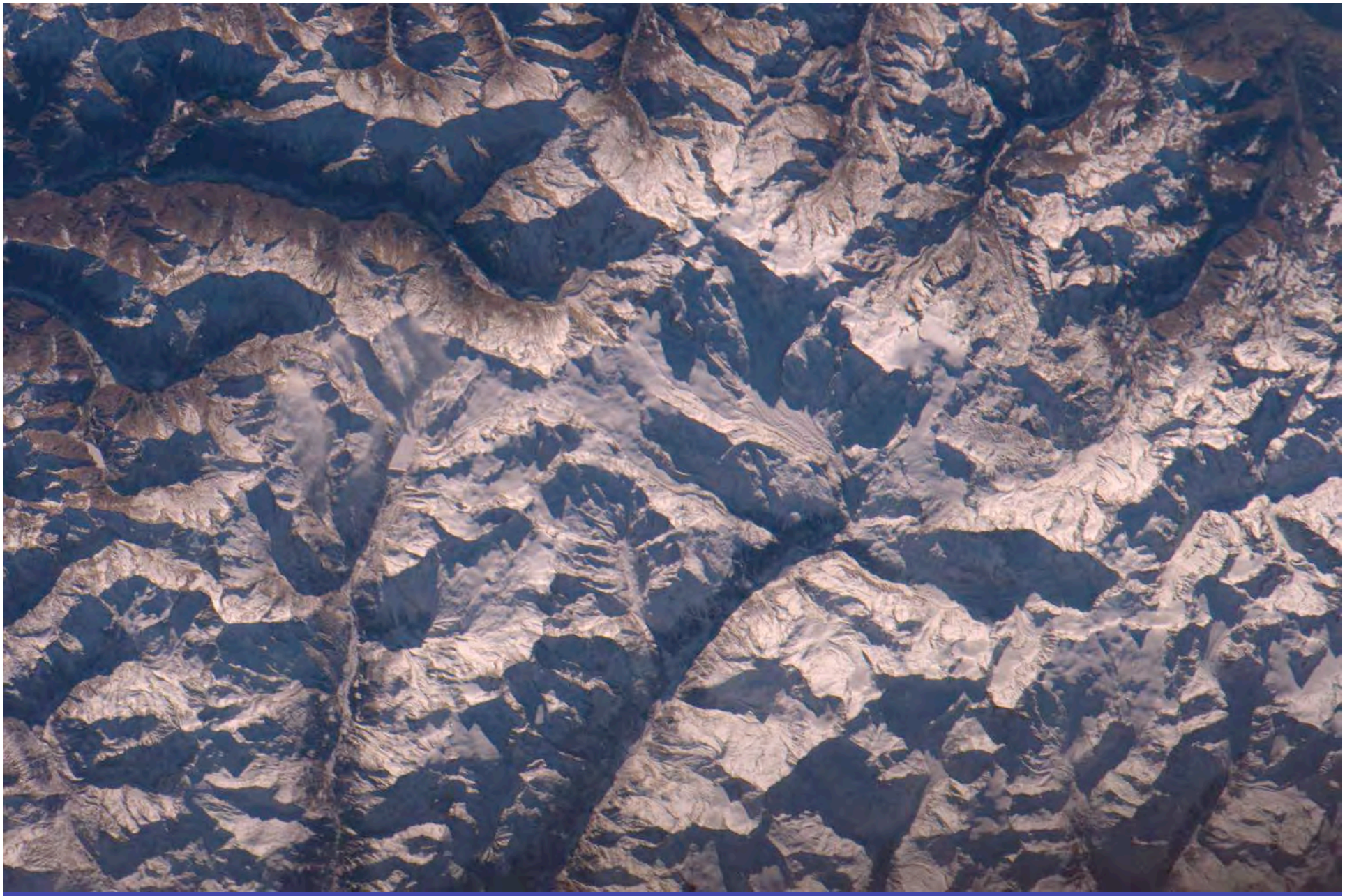

Alps: Zermatt, the Matterhorn

http://eol.jsc.nasa.gov/

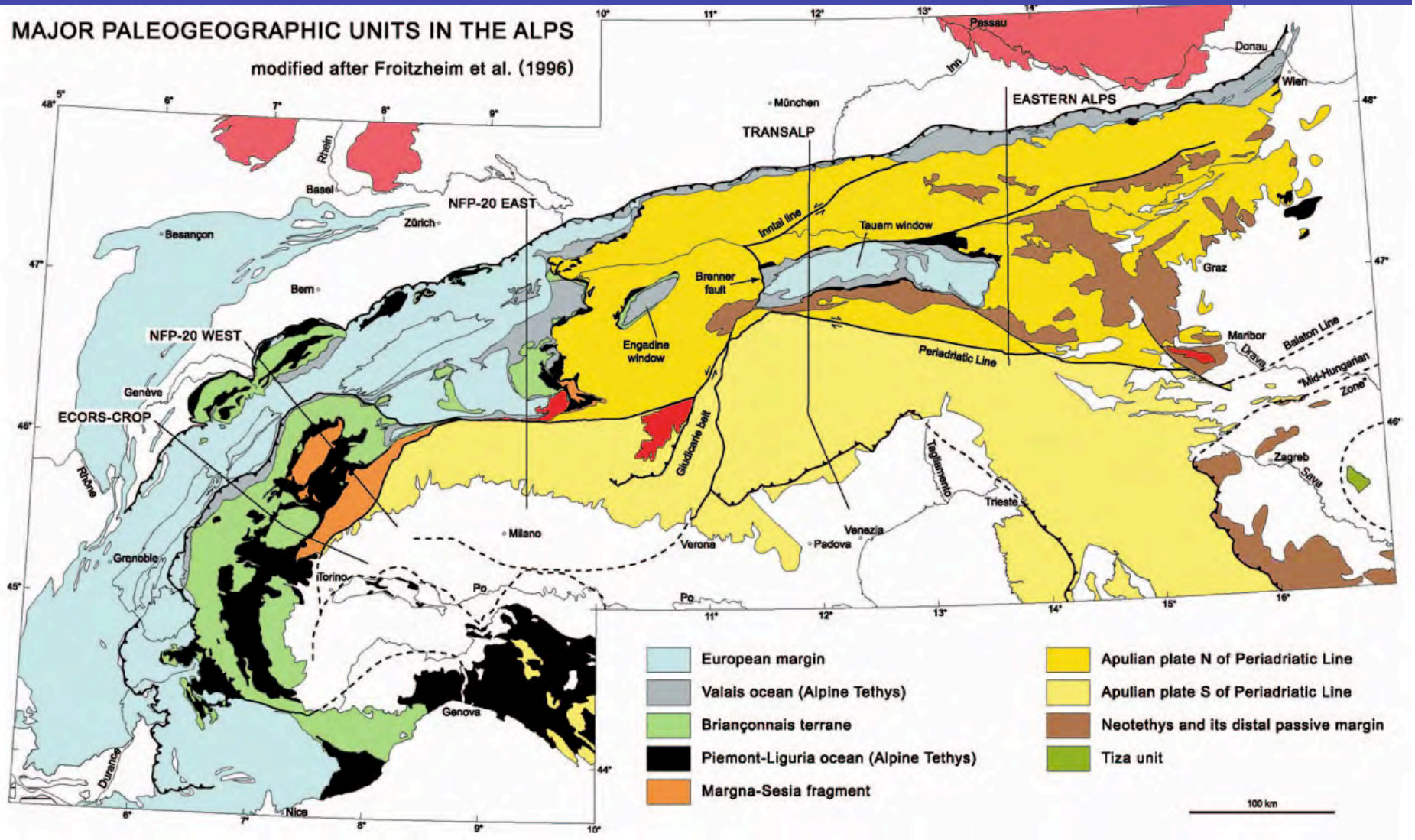

Fig. 1. Map of the major paleogeographic and tectonic units in the Alps.

Schmidt et al 2004

Alpine Crustal Profiles

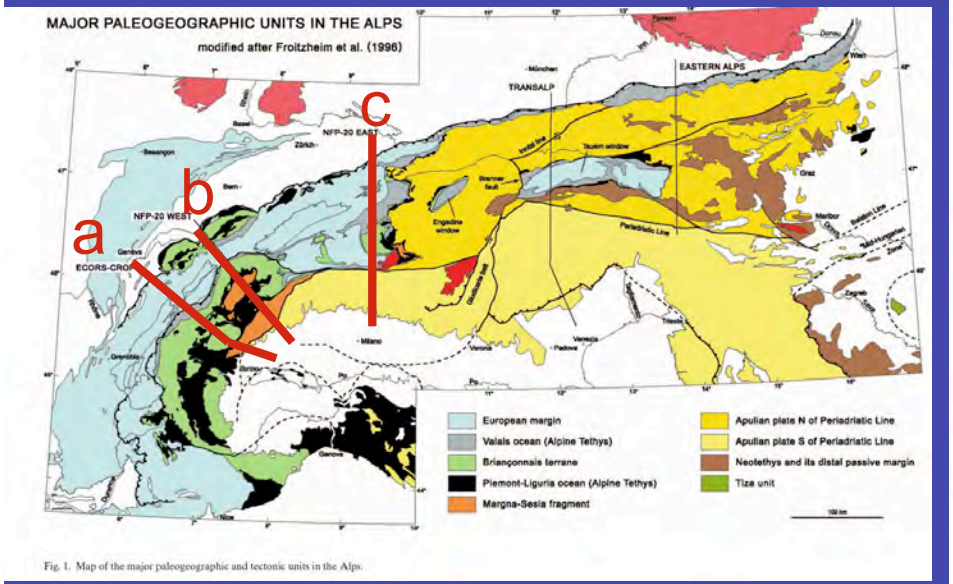

Fig. 1. Map of the major paleogeographic and tectonic units in the Alps.

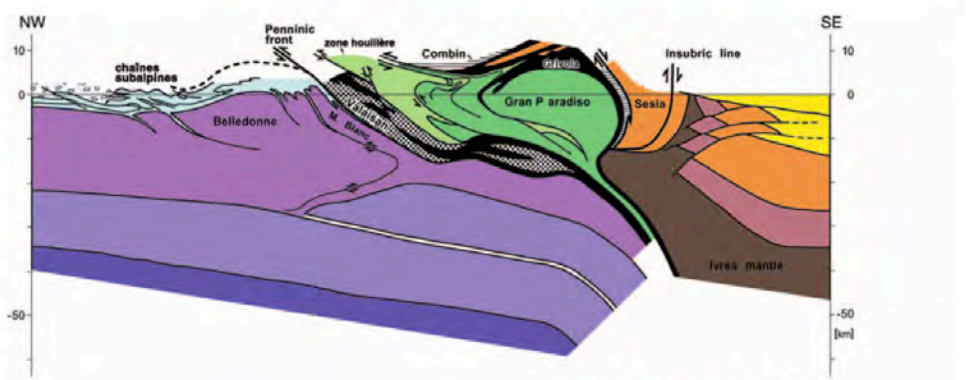

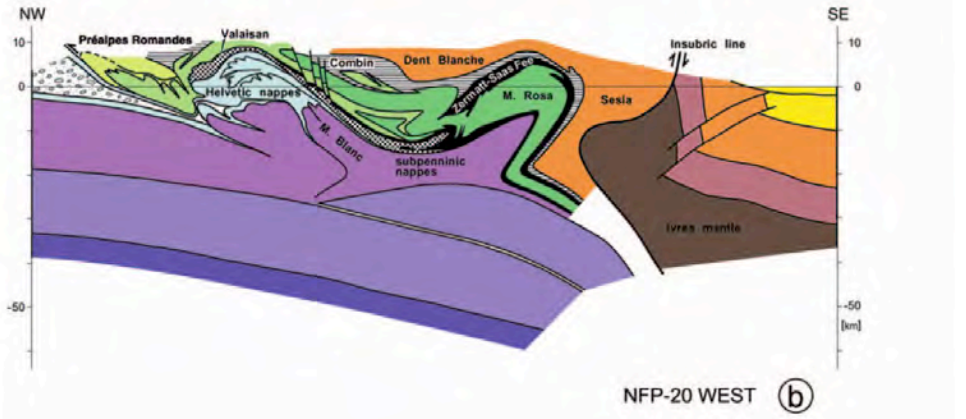

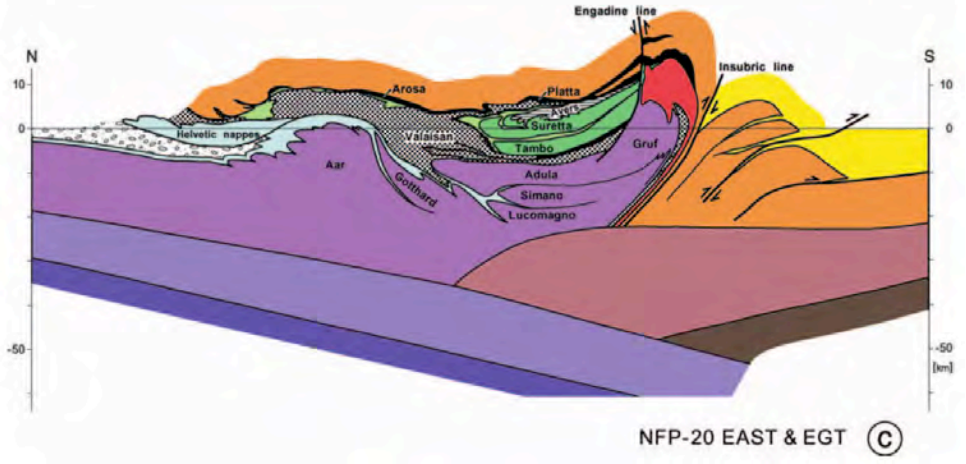

Schmidt et al 2004

Alpine Crustal Profiles

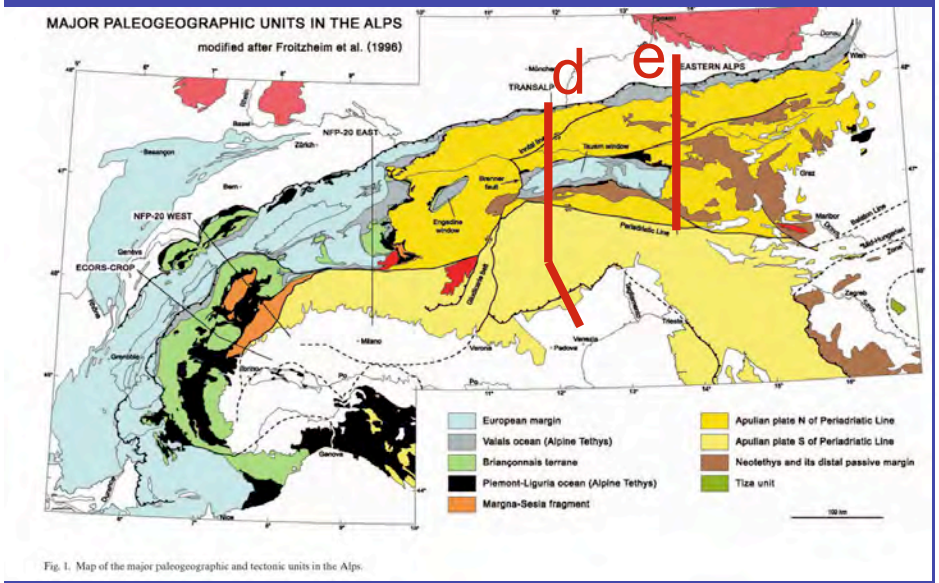

Fig. 1. Map of the major paleogeographic and tectonic units in the Alps.

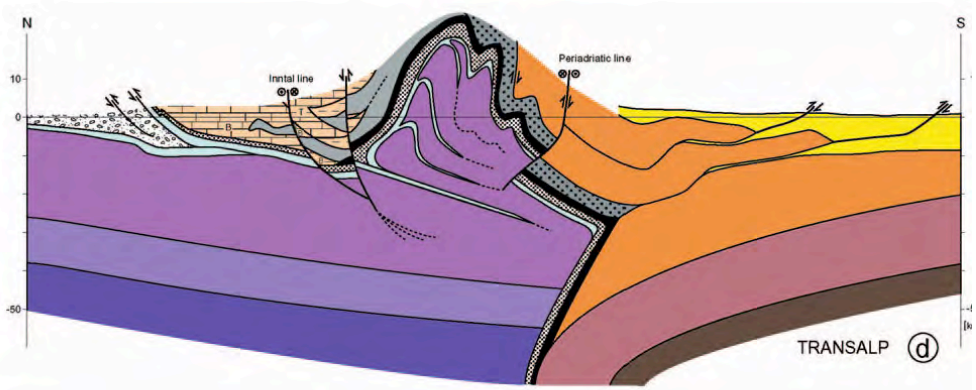

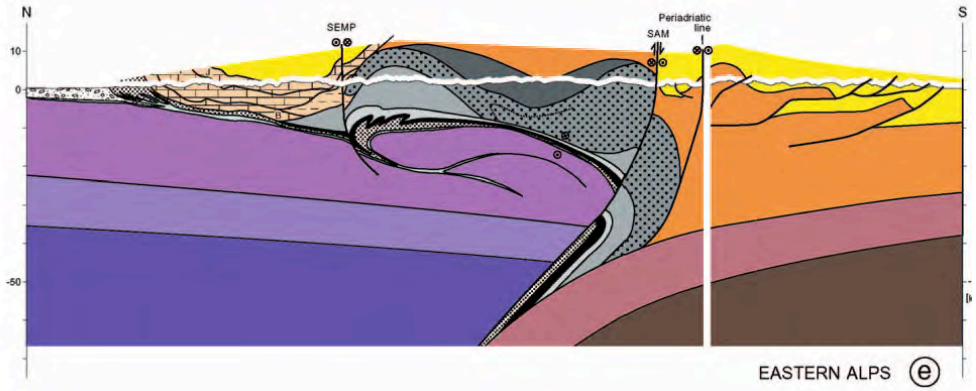

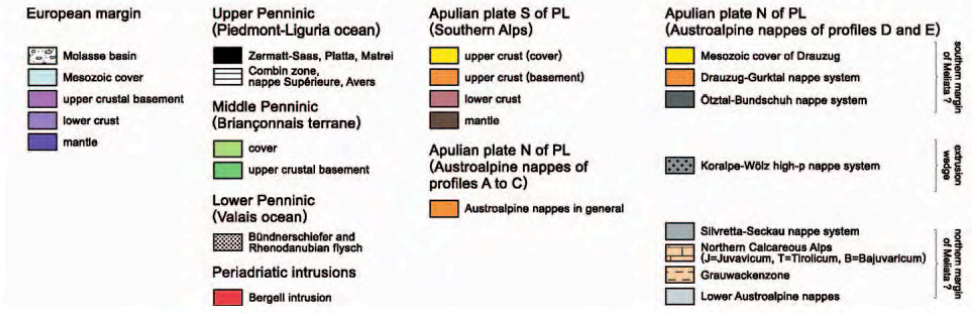

Schmidt et al 2004

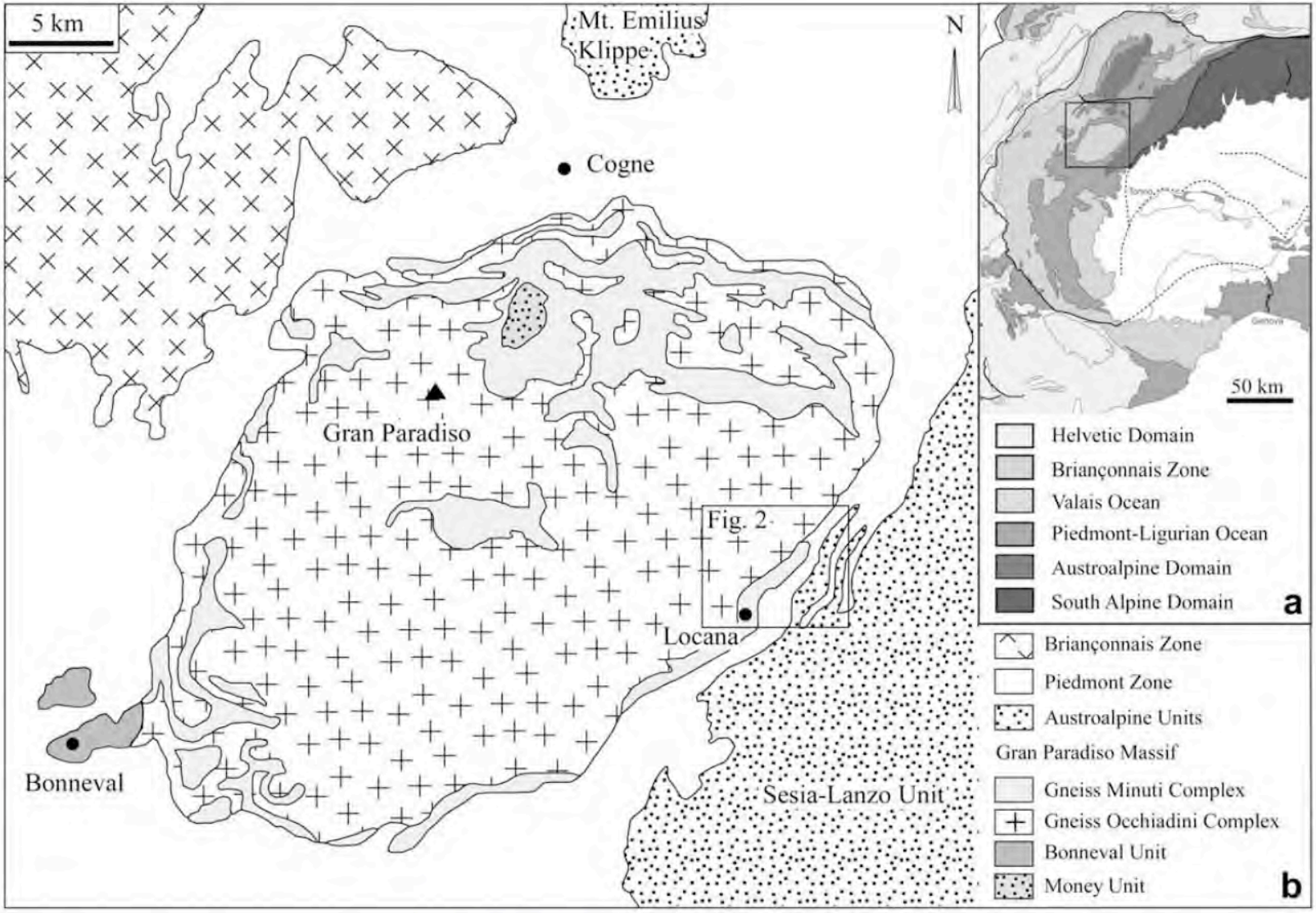

1. (a) Tectonic map of the Western Alps (modified after Schmid et al., 2004). (b) Simplified geological map of the Gran Paradiso Massif and surrounding units (modified after ppagnoni and Lombardo, 1974)

Gasco et al 2010

Gasco et al 2010

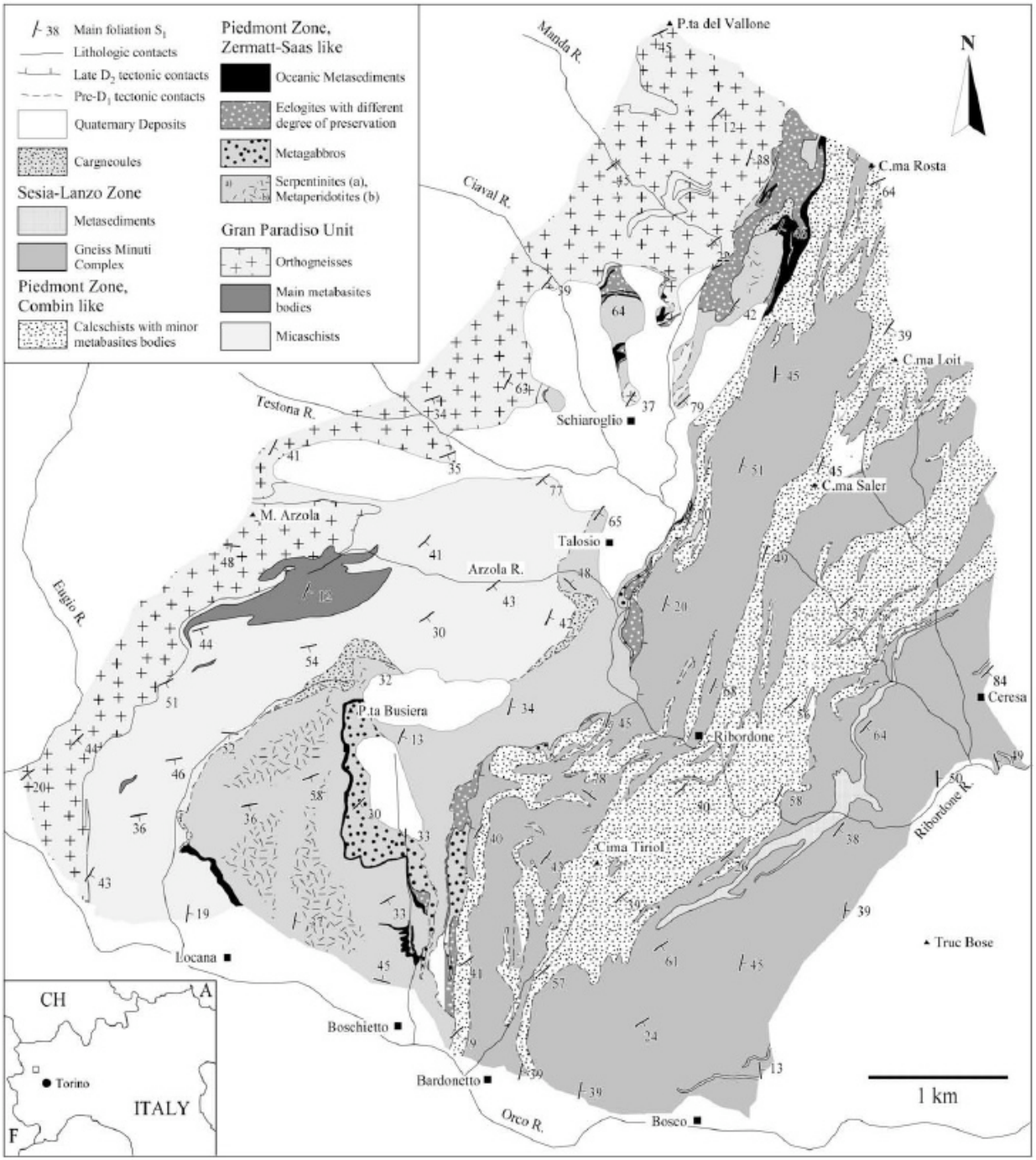

Fig. 2. Simplified geological map of the study area located at the western border of the Gran Paradiso Unit.

Evolution of the mineral assemblages respect to the structural and metamorphic setting in the main lithologies occurring in the different tectonic units.

Structural evolution	Metamorphic conditions	Lower tectonic unit (eclogite facies relics)						Metamorphic conditions	Upper tectonic unit (only greenschist facies assemblages)		
		Gran Paradiso Unit			*Piedmont Zone*				*Piedmont Zone*		*Sesia–Lanzo Zone*
					Zermatt–Saas Unit				*Combin Unit*		*Gneiss Minuti Complex*
		Micaschists	Metabasites	Orthogneisses (whiteschists)	Serpentinites (metaperidotites)	Metagabbros	Metabasites		Calcschists	Greenstones	Gneisses (metagranitoids)
Pre-Alpine		Enclaves in orthogneisses	Magmatic structures	Kfs, Qtz, Bt, Pl	(Ol, Cpx, Opx, Spl) (Ol, Chl, Am, Mag)	Magmatic structures	–		–	–	Magmatic structures
Pre-S_1	Eclogite facies	Grt, Gln, Wm, Qtz, Rt	Omp, Grt, Gln, Zo, Wm, Rt	(Wm, Qtz, Chl, Cld, Ky, Tlc, Grt)	–	Omp, Gln, Grt	Omp, Grt, Gln, Wm, Zo/Ep, Rt	Greenschist facies	Wm, Cal, Qtz, Chl	–	Wm, Qtz, Chl, Ep, Act; (Zo, Rt)
S_1	Middle-*P* greenschist to epidote–albite amphibolite facies	Wm, Qtz, Hbl, Ab, Grt, Zo, Rt	Ca–Na Am, Zo, Wm, Chl, Ab, Rt	Wm, Qtz, Ab, Ep, Spn (Qtz, Wm, Chl)	Srp, Chl, Ol, Di	Am, Zo, Wm, Chl, Rt	Ca–Na Am, Zo, Wm, Chl, Rt	Greenschist facies	Wm, Qtz, Cal, Spn, Chl	Act, Ab, Ep, Chl, Spn	Wm, Qtz, Ab, Ep/Czo, Chl, Act, Spn
S_2	Greenschist facies	Qtz, Wm, Chl, Ab, Spn	–	–	Srp	–	–		Wm, Chl, Qtz, Spn	–	Wm, Chl, Act
S_3	Low-grade metamorphic conditions	–	–	–	Srp	–	–		Wm, Cal, Qtz	–	–
S_4 (ECC)	Ductile to brittle	Qtz, Wm, Bt	–	–	Srp	–	–		Wm, Cal, Qtz	–	Qtz, Wm, Bt, Spn

Sketch of the tectono-metamorphic evolution of the studied units.

	Lower Tectonic Element (eclogite facies relics)		Upper Tectonic Element (only greenschist facies assemblages)	
	Gran Paradiso Unit	*Zermatt-Saas Unit*	*Combin Unit*	*Sesia-Lanzo GMC*
pre-D_1	eclogite facies	eclogite facies	greenschist facies	greenschist facies
old tectonic contacts	blueschist facies		greenschist facies	
D_1	middel-P greenschist to epidote-albite amphibolite facies		greenschist facies	
D_2	greenschist facies		greenschist facies	
OSZ late-D_2	greenschist facies			
D_3	low-grade metamorphic conditions			
D_4 (ECC)	ductile (low-grade metamorphic conditions) to brittle			

Gasco et al 2010

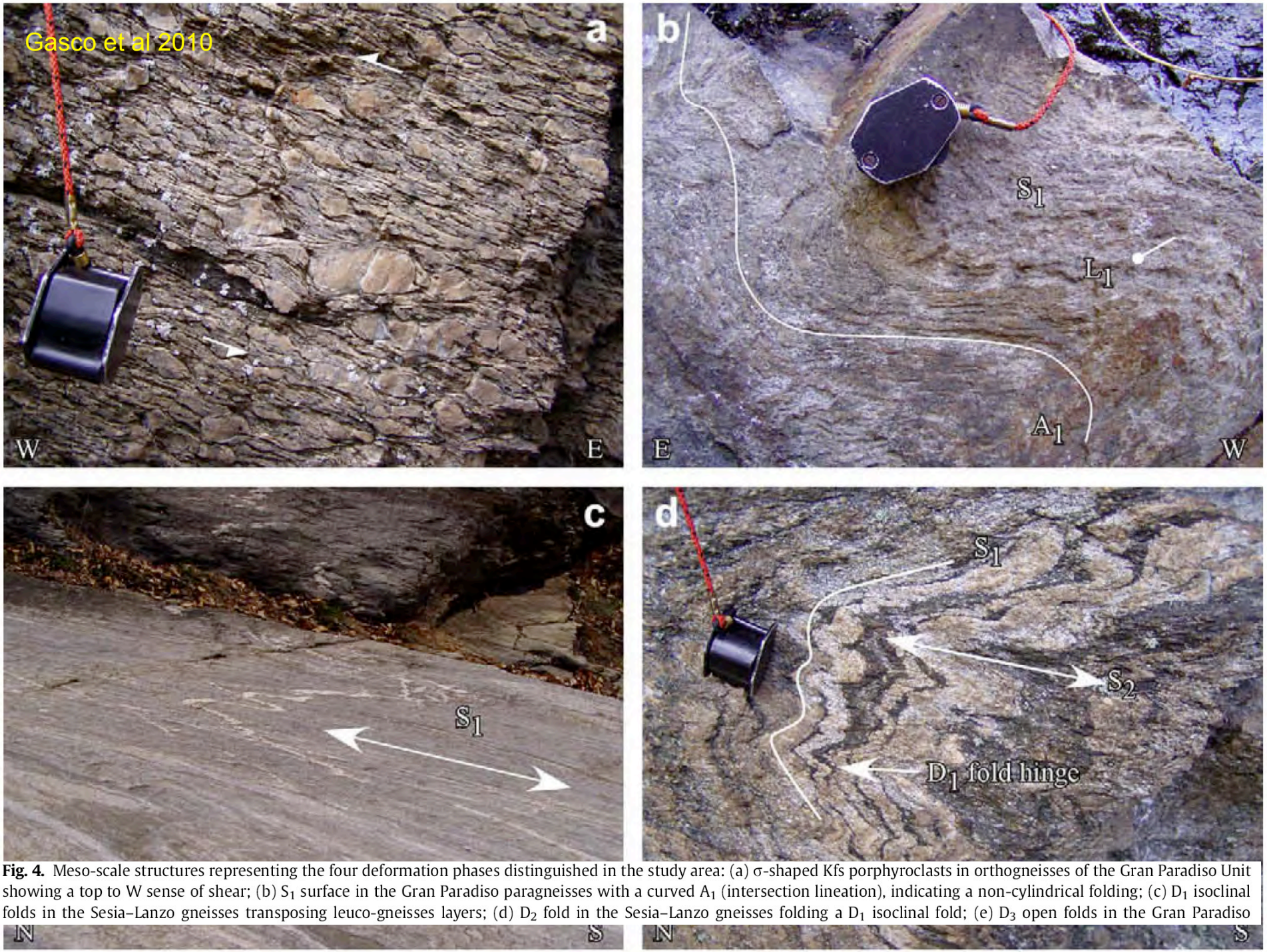

Fig. 4. Meso-scale structures representing the four deformation phases distinguished in the study area: (a) σ-shaped Kfs porphyroclasts in orthogneisses of the Gran Paradiso Unit showing a top to W sense of shear; (b) S_1 surface in the Gran Paradiso paragneisses with a curved A_1 (intersection lineation), indicating a non-cylindrical folding; (c) D_1 isoclinal folds in the Sesia–Lanzo gneisses transposing leuco-gneisses layers; (d) D_2 fold in the Sesia–Lanzo gneisses folding a D_1 isoclinal fold; (e) D_3 open folds in the Gran Paradiso

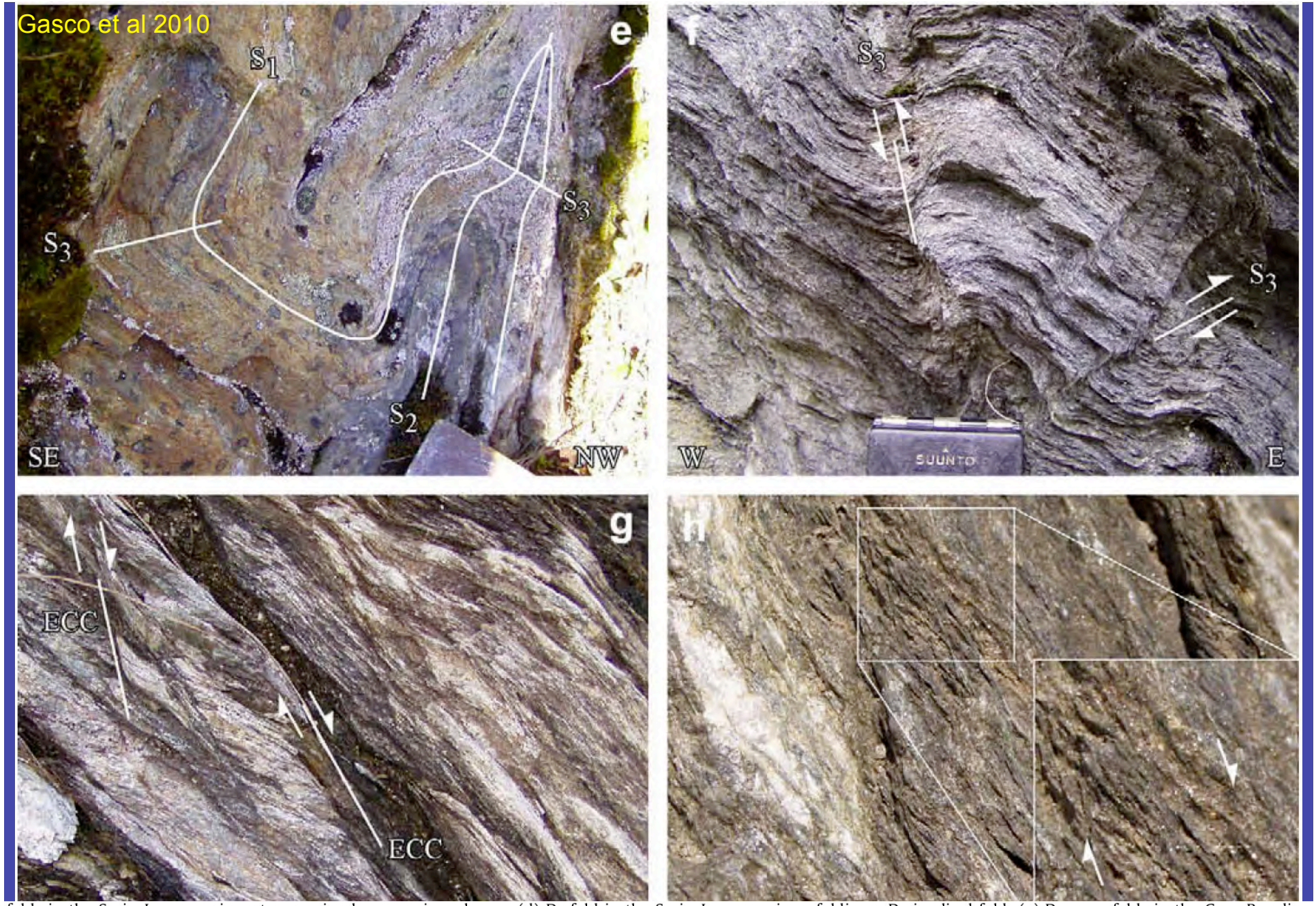

folds in the Sesia–Lanzo gneisses transposing leuco-gneisses layers; (d) D_2 fold in the Sesia–Lanzo gneisses folding a D_1 isoclinal fold; (e) D_3 open folds in the Gran Paradiso paragneisses folding a tight to isoclinal D_2 fold; (f) D_3 box fold in the Combin-like calcschists with S_3 surfaces defined by a spaced and discontinuous reverse-slip C′ types shear bands; (g) discontinuous Extensional Crenulation Cleavage in the Zermatt–Saas serpentinites; (h) S–C type shear bands showing a top to E sense of shear in mylonitic calcschists along the tectonic contact between the Upper Tectonic Element and the Lower one.

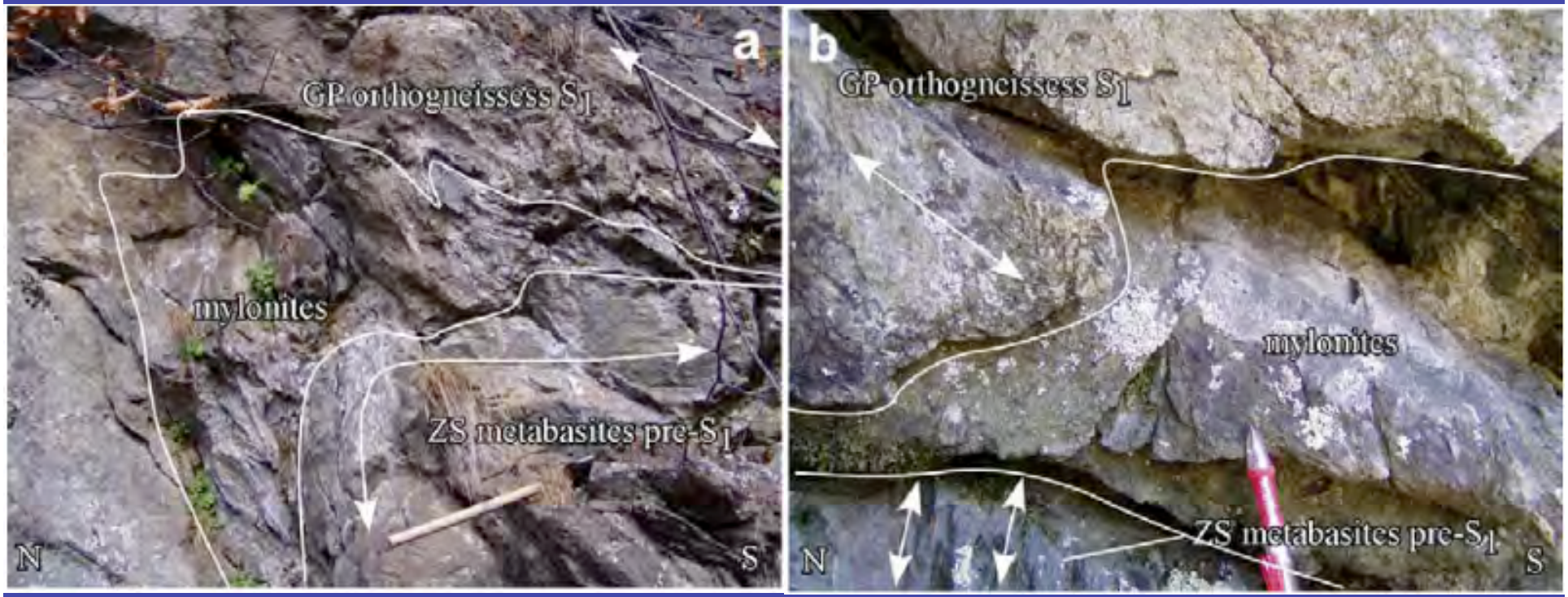

Fig. 6. Structural and metamorphic relationships between the Gran Paradiso orthogneisses and the Zermatt–Saas eclogites: (a) orthogneisses show a well-developed S_1 foliation while metabasites preserve a pre-S_1 foliation; (b) eclogite facies pre-S_1 foliation is preserved in metabasites and is cut by mylonites.

Gasco et al 2010 figure 6

Gasco et al 2010

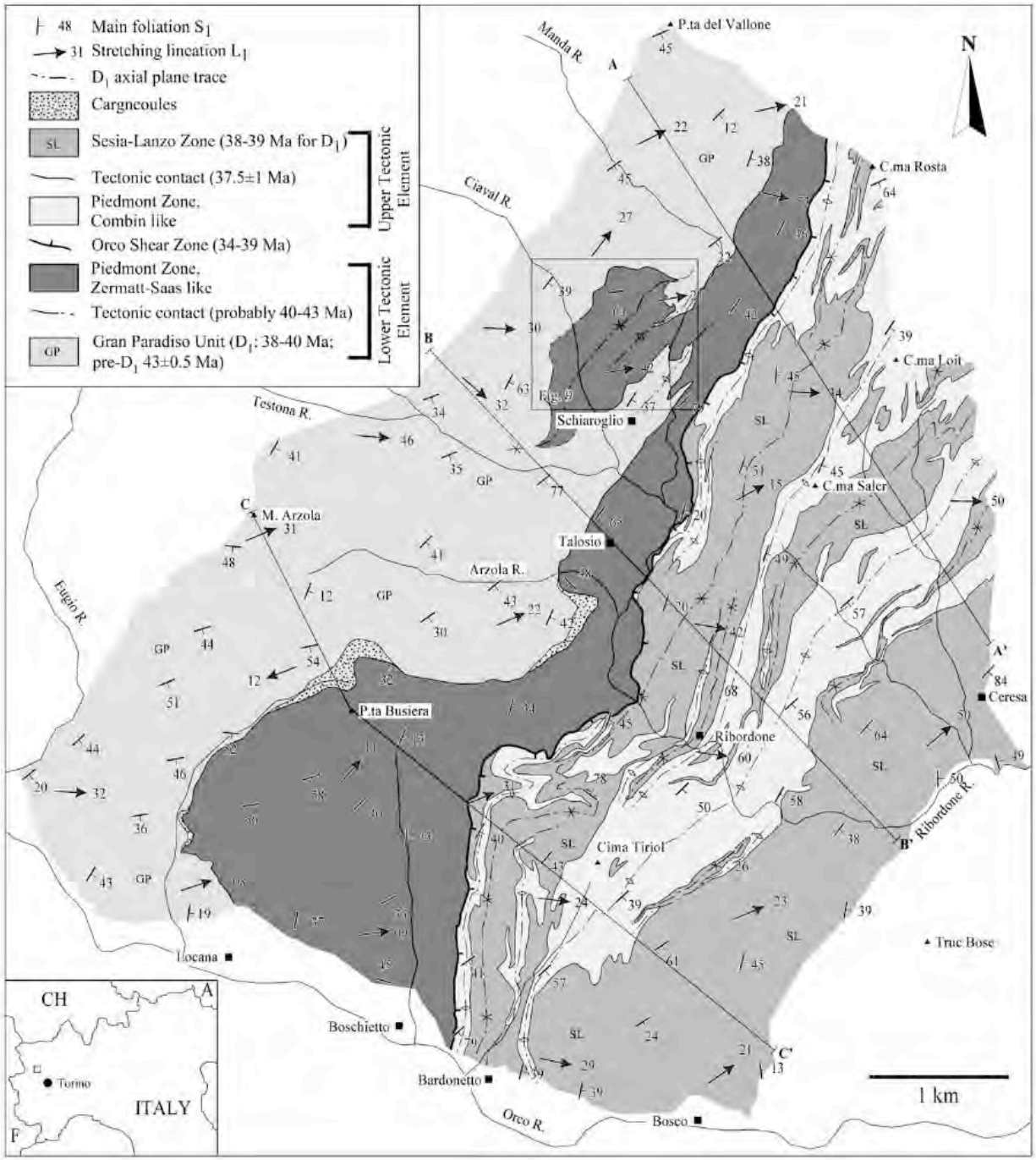

Fig. 7. Simplified structural map of the study area with some structural features of the D_1 event. Only the different palaeo-geographic units are distinguished to show their structural relationship (geochronological data from Inger et al., 1996; Inger and Ramsbotham, 1997; Meffan-Main et al., 2004).

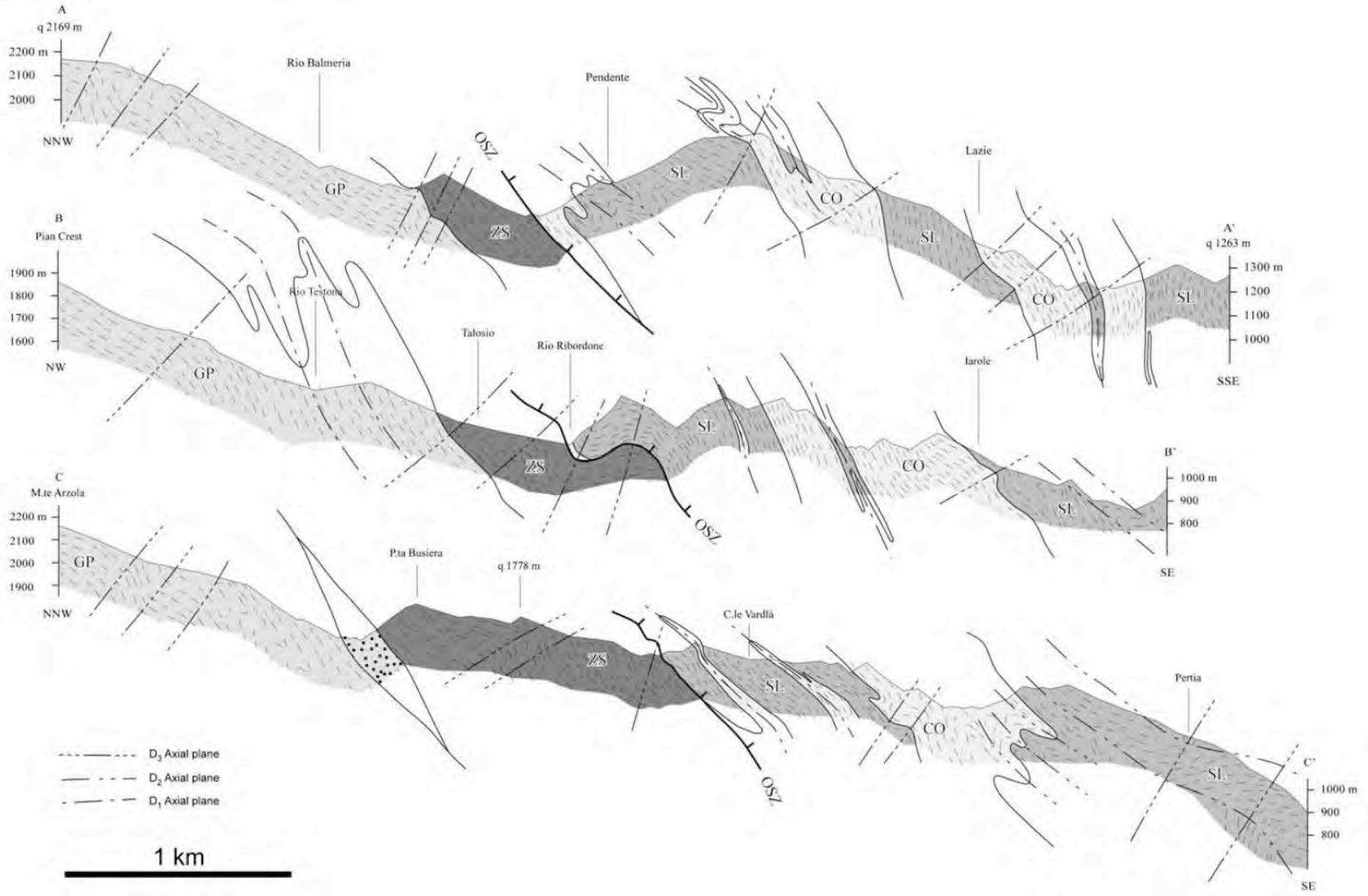

Fig. 8. Cross-sections representing the structural relationships between the different tectonic units (see text for explanation). GP, Gran Paradiso Unit; ZS, Zermatt–Saas Unit; CO, Combin Unit; SL, Sesia–Lanzo Gneiss Minuti Complex; OSZ, Orco Shear Zone. Legend as in Fig. 7.

Gasco et al 2010

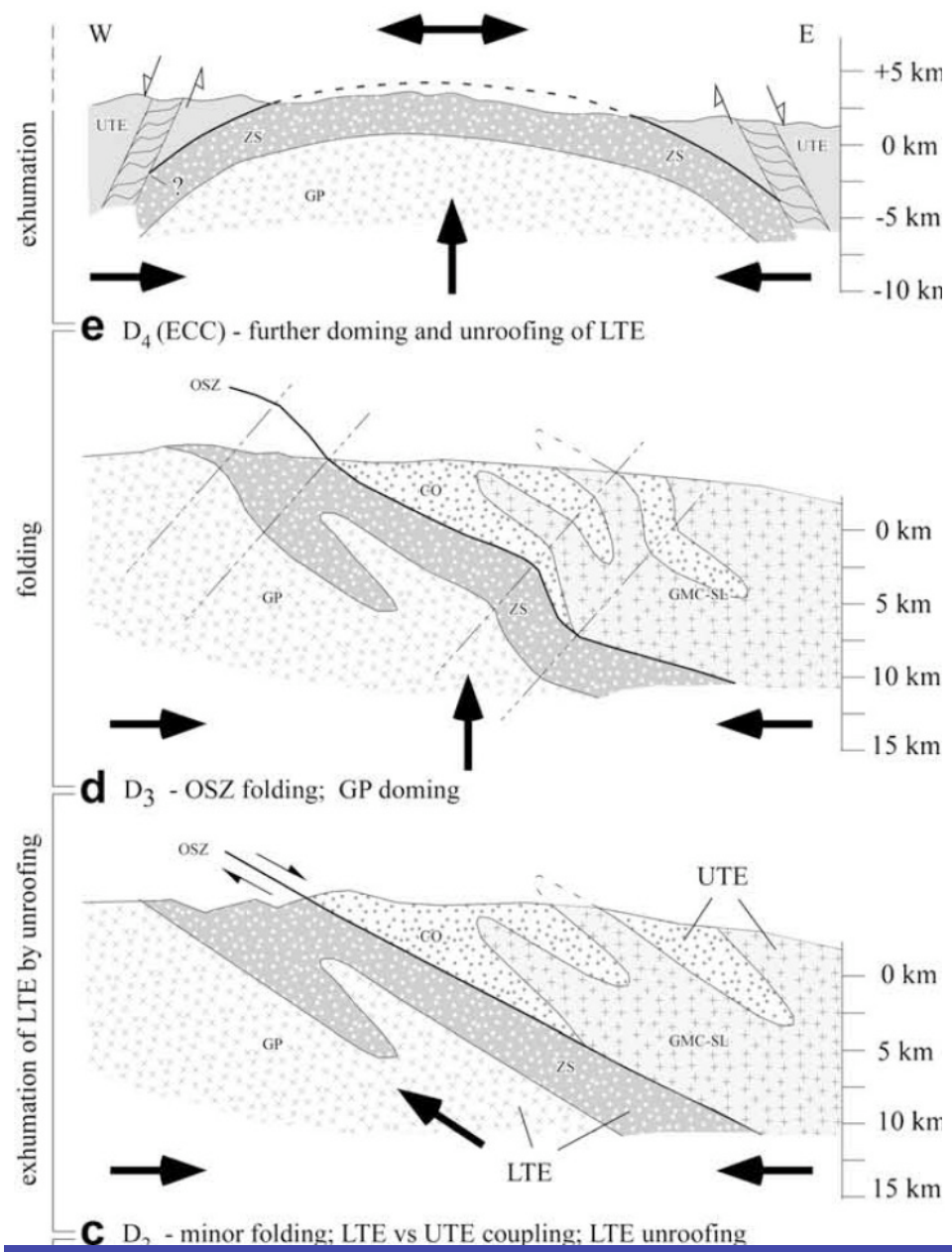

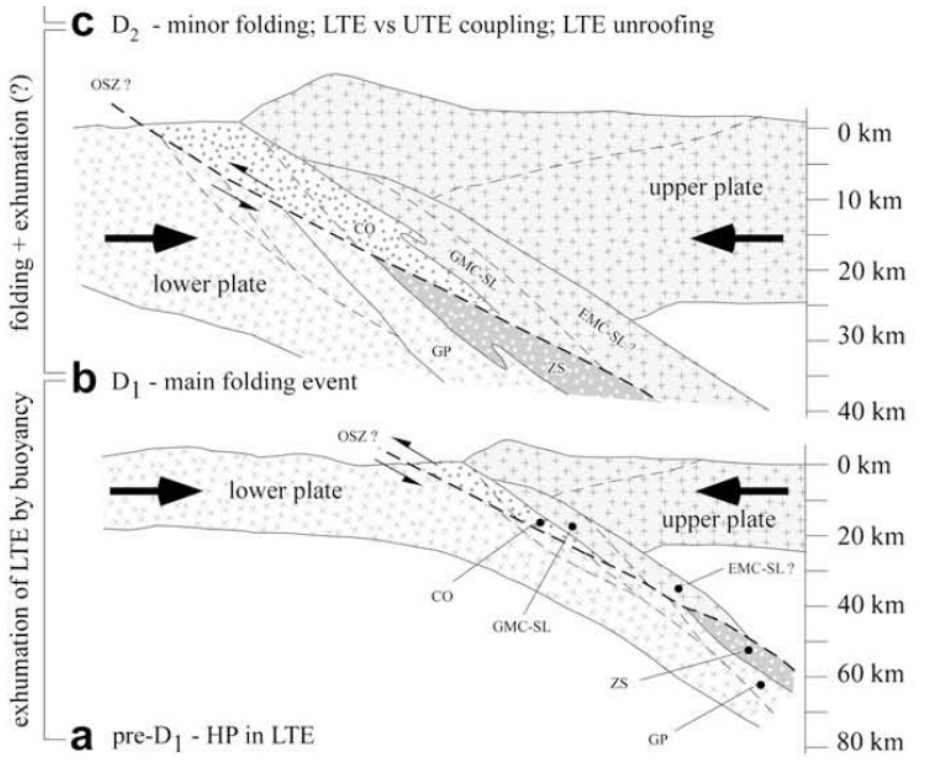

Fig. 10. W–E cross-sections representing the structural history of the Orco Valley geological transect related to its possible geodynamic evolution. OSZ, Orco Shear Zone; EMC-SL, Eclogitic Micaschists Complex, Sesia–Lanzo; GMC-SL, Gneiss Minuti Complex, Sesia–Lanzo; CO, Combin Unit; ZS, Zermatt–Saas Unit; GP, Gran Paradiso Unit. LTE, Lower Tectonic Element; UTE, Upper Tectonic Element. (a) pre-D_1 stage and HP metamorphism in the LTE. The position of the OSZ is indicated and probably accommodated reverse-slip movement. (b) D_1 stage represents the main folding event resulting in a well-developed regional foliation in both the UTE and the LTE. (c) D_2 stage is linked to minor folding (not shown) and to the exhumation of the LTE along the OSZ that cuts D_1 structures. (d) D_3 stage folded the OSZ and caused the doming of the Gran Paradiso Unit. (e) D_4 stage is associated to the Extensional Crenulation Cleavage (ECC) on both side of the LTE and probably represents the onset of gravitational collapse.

Gasco et al 2010

PRESENT DAY

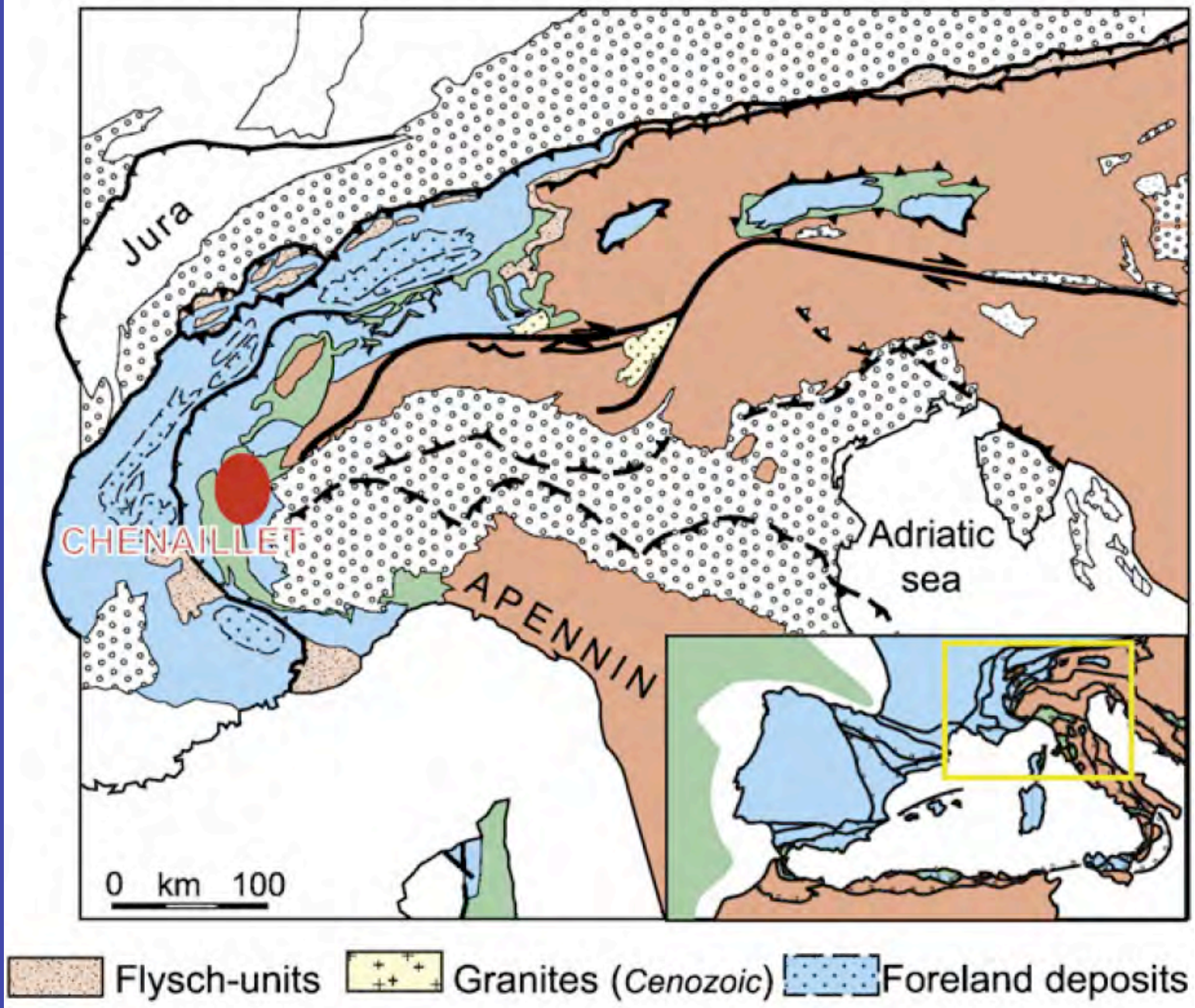

Manatschal
et al 2011

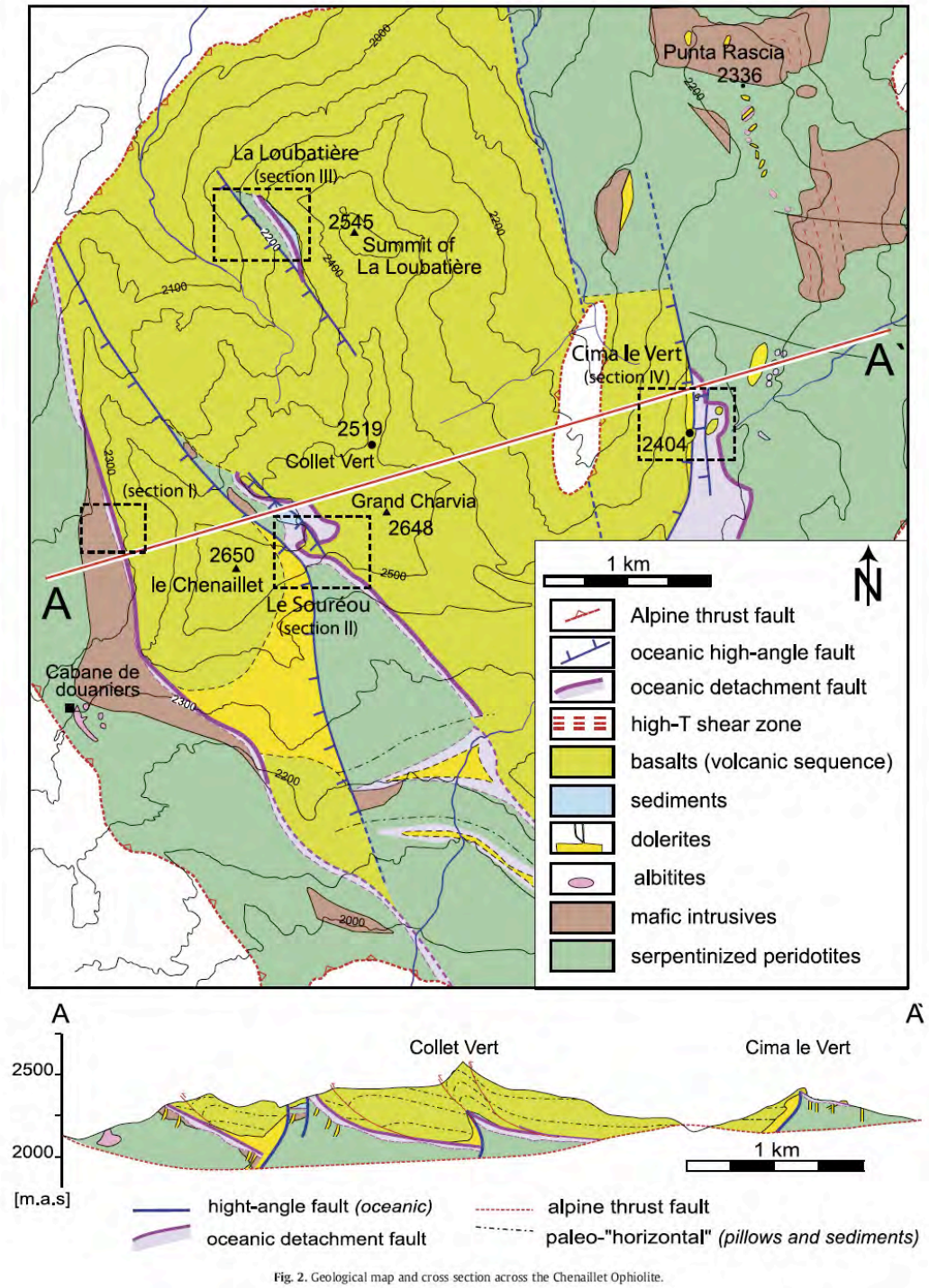

Fig. 2. Geological map and cross section across the Chenaillet Ophiolite.

Manatschal
et al 2011

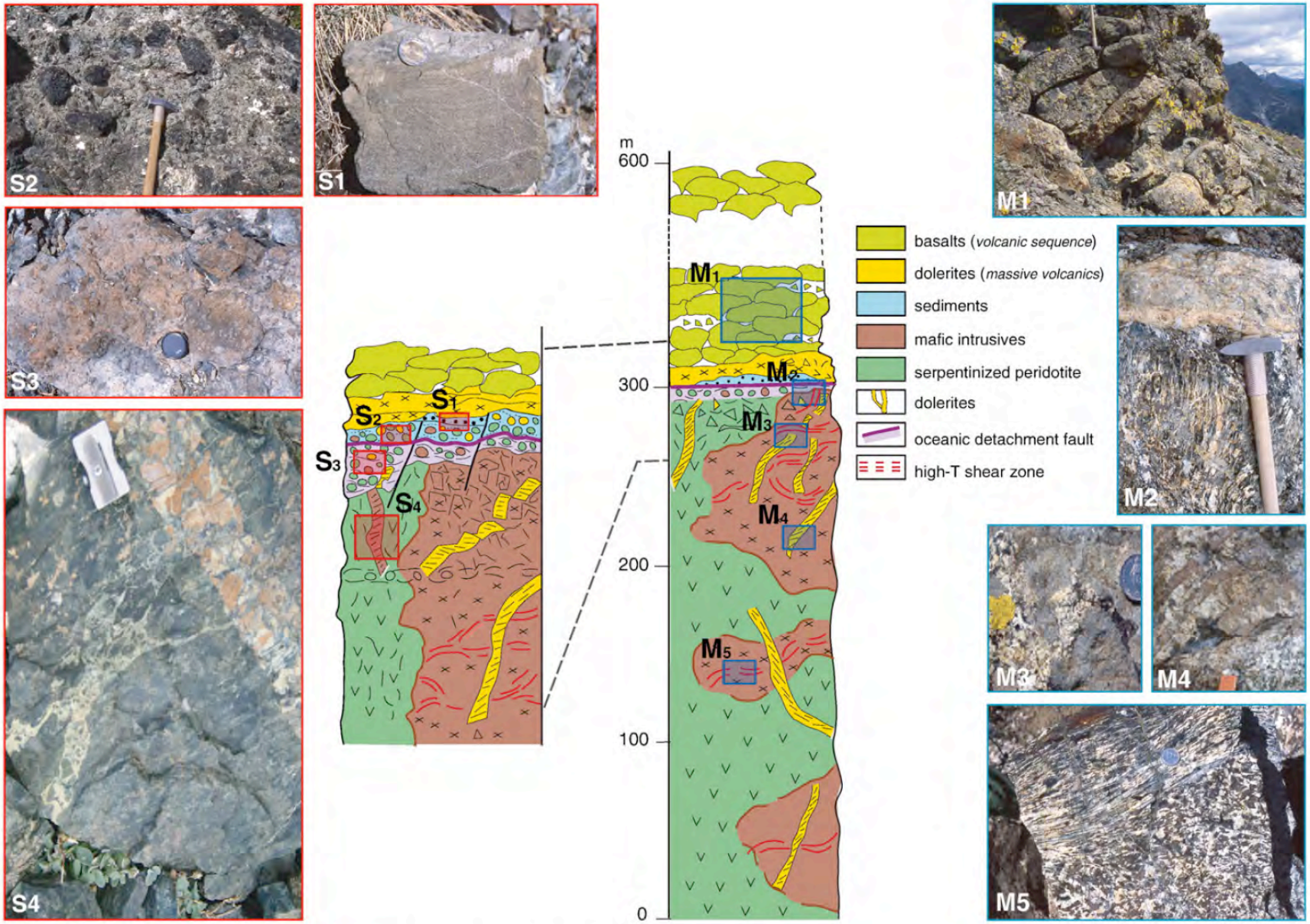

Fig. 3. Synthetic stratigraphic section showing the lithologies as well as the nature of their contacts. Section to the left shows a detailed view of the contact between the exhumed serpentinized mantle and intrusive mafic rocks, and the overlying sediments and volcanic section. This contact corresponds to an oceanic detachment fault. Photographs: S1) graded and laminated serpentinite sandstone (La Loubatière); S2) ophicalcite consisting of a calcified serpentinite breccia (E of Chenaillet); S3) serpentinite gouge (E of Chenaillet); S4) serpentinized peridotite with gabbro vein overprinted by brittle deformation (La Loubatière); M1) Pillow basalts (W of Chenaillet); M2) high-temperature shear zone in gabbro cut by low-temperature, altered fault zone representing the oceanic detachment fault (NW of Chenaillet); M3) syn-magmatic relation between dolerites and gabbros (W of Chenaillet); M4) high-temperature shear zone in the gabbro (N of Le Souréou).

Manatschal et al 2011

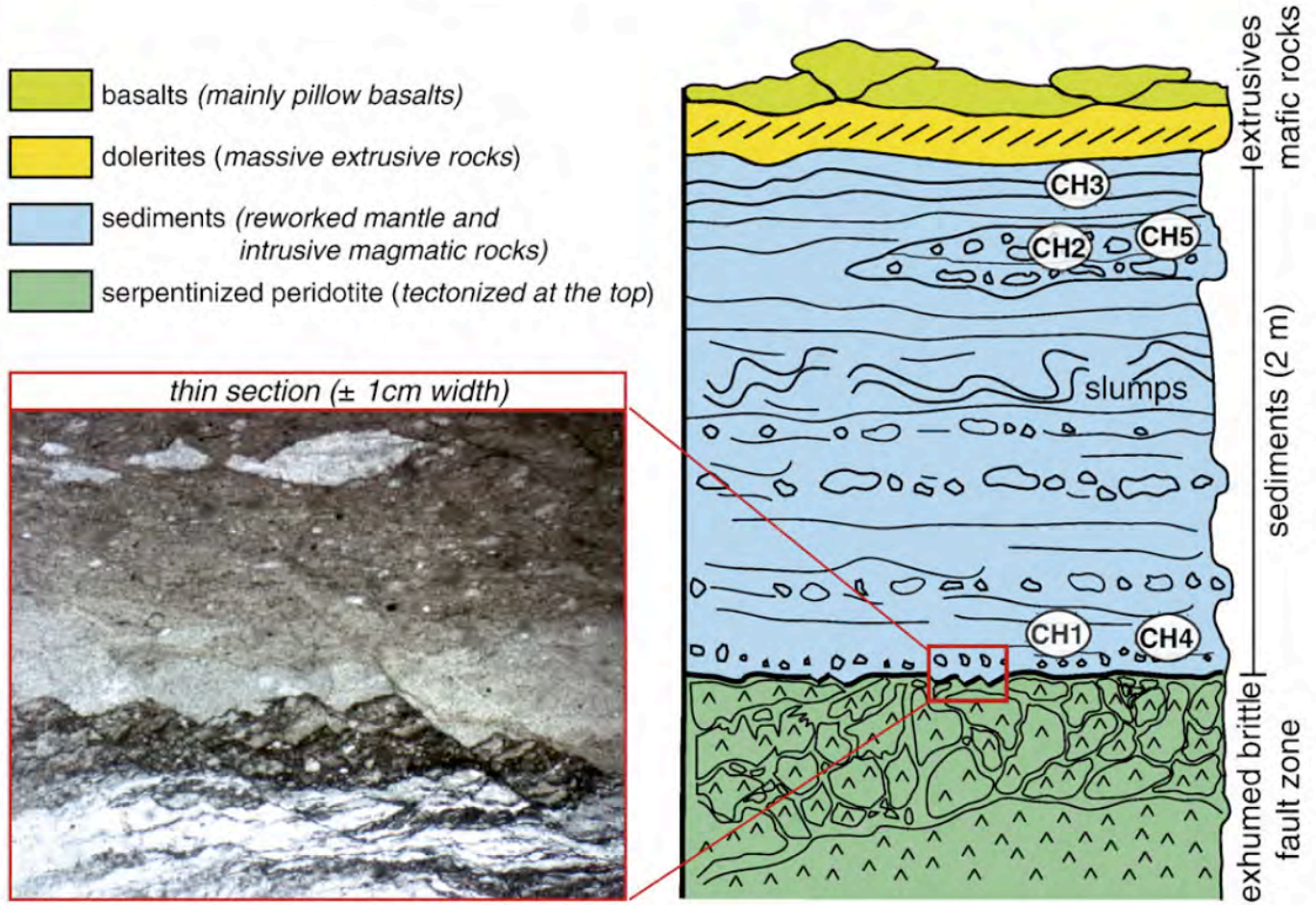

Fig. 4. Sedimentary sequence observed at La Loubatière overlying exhumed and tectonized mantle with a stratigraphic contact. The thin section photograph to the left shows the sediments overlying a foliated serpentinite. The contact itself is cut by high-angle faults that are sealed by sediments in the upper part of the section. Therefore, we interpret these high-angle faults as oceanic high-angle faults. Note that within the sediments, slumps occur, indicating that deposits were on a slope. The sediments are overlain by extrusive mafic rocks.

Manatschal et al 2011

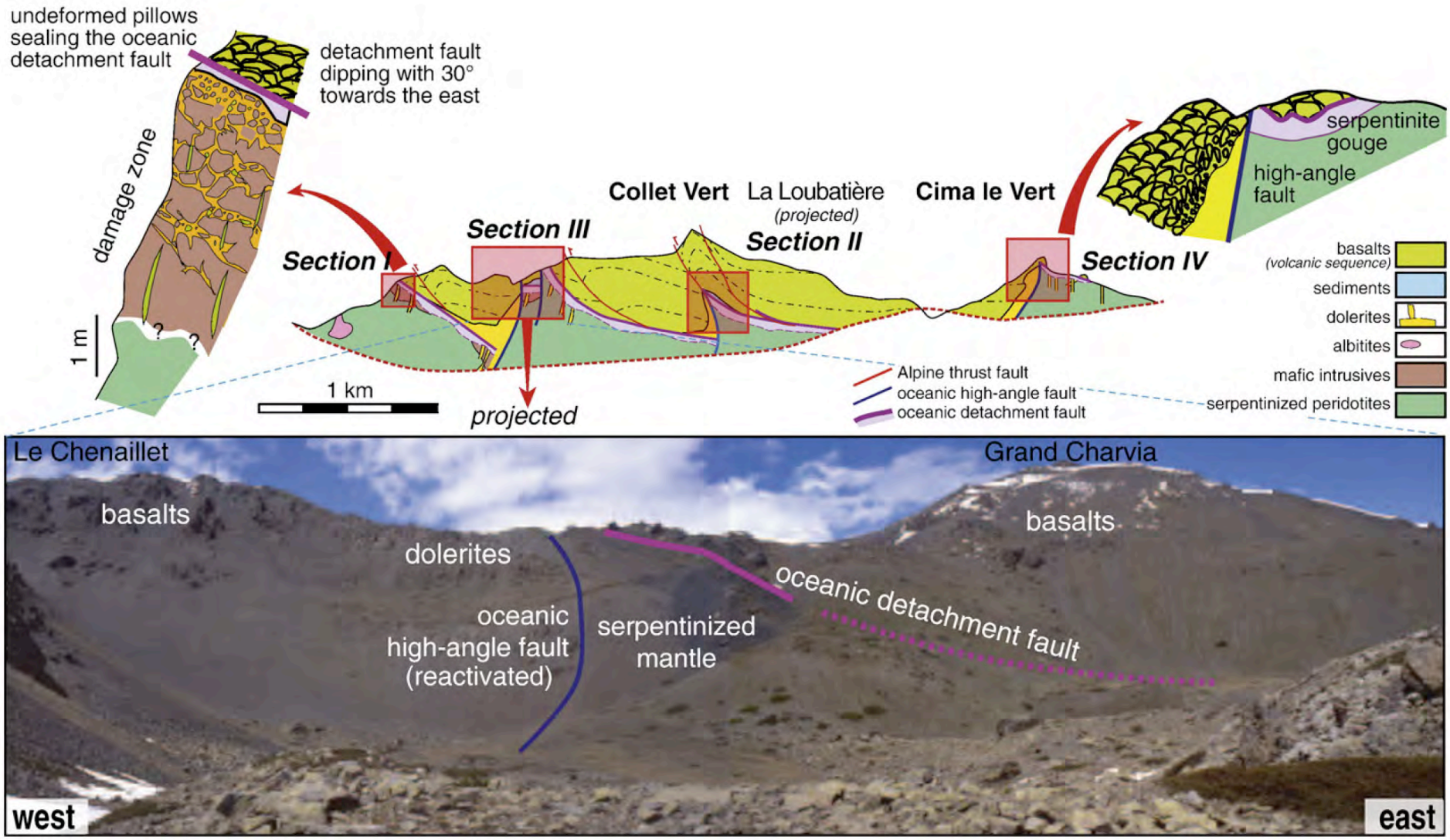

Fig. 6. Major structural observations made in the Chenaillet Ophiolite. Cross section is taken from Fig. 2 and for locations see map in Fig. 2. Sections I to IV show the relations between basement (serpentinites and gabbros) and cover (sediments and volcanic sequence): section I is localted north of Chenaillet and show the transition from deformed gabbros at the top of the basement into an oceanic detachment fault that is overlain by pillow basalts; section II is located at Le Souréou and it preserves the relation between and oceanic detachment fault, high-angle faults and basalts and sediments; section III is located at La Loubatière where an oceanic detachment fault is directly overlain by sediments and basalts (see also Fig. 4); section IV corresponds to Cima le Vert, where an equivalent situation to that observed at Le Souréou exists.

Manatschal et al 2011

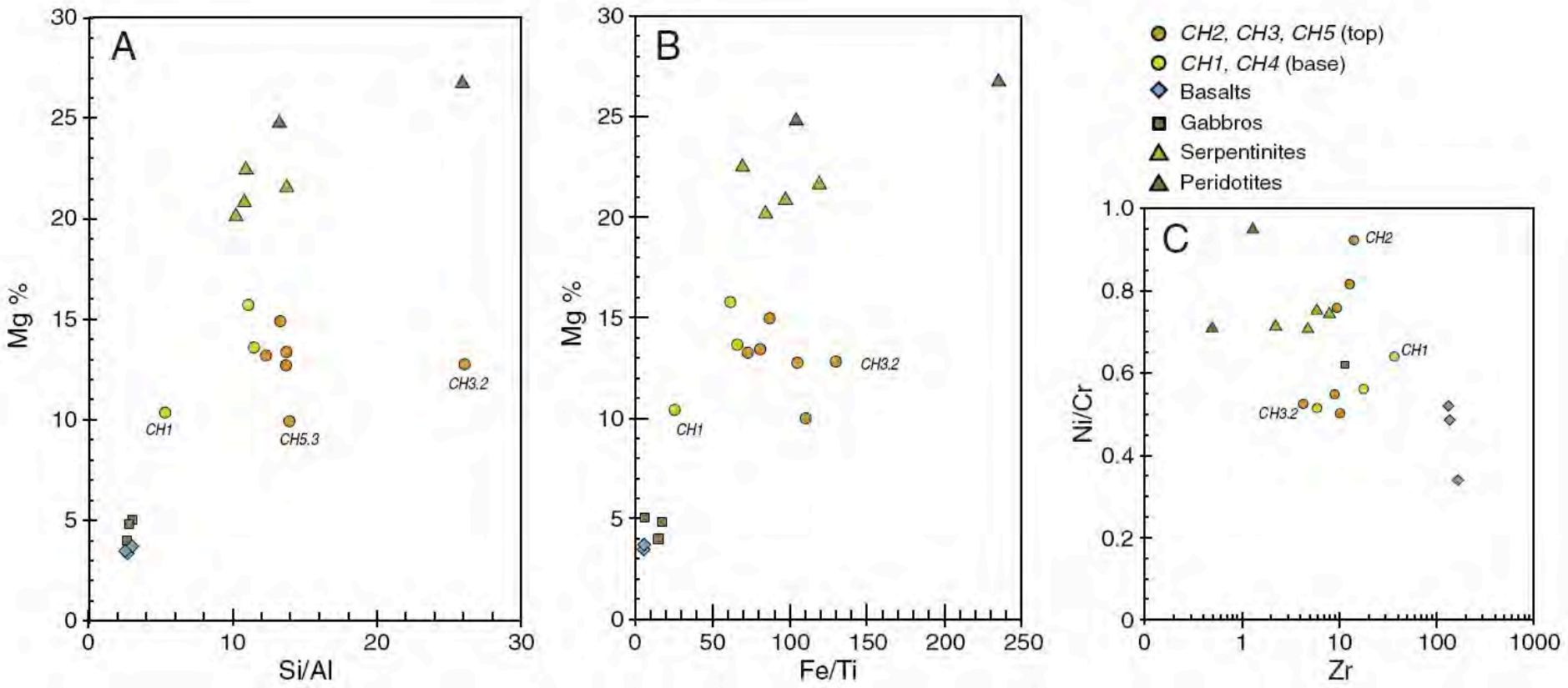

Manatschal et al 2011

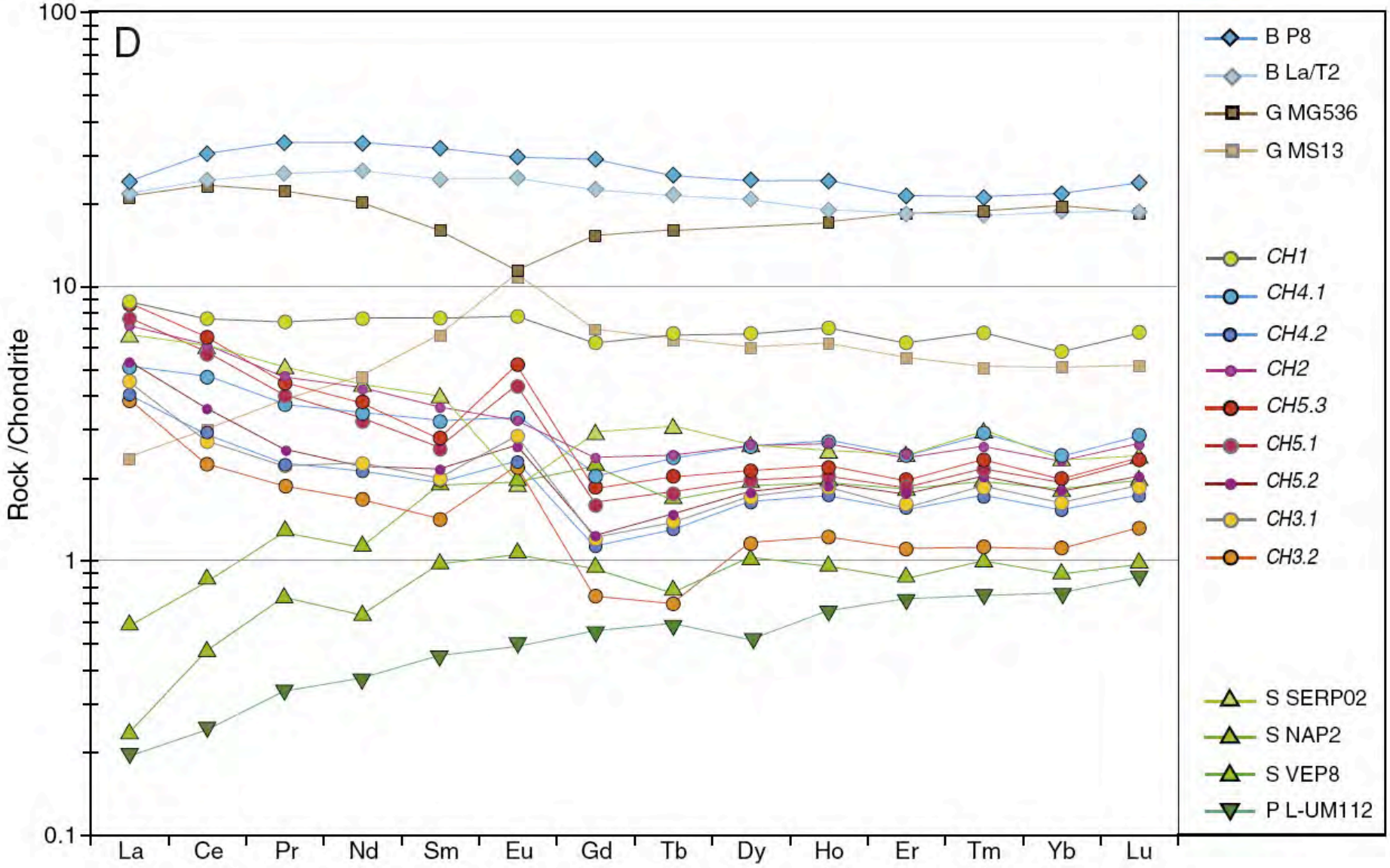

Manatschal et al 2011

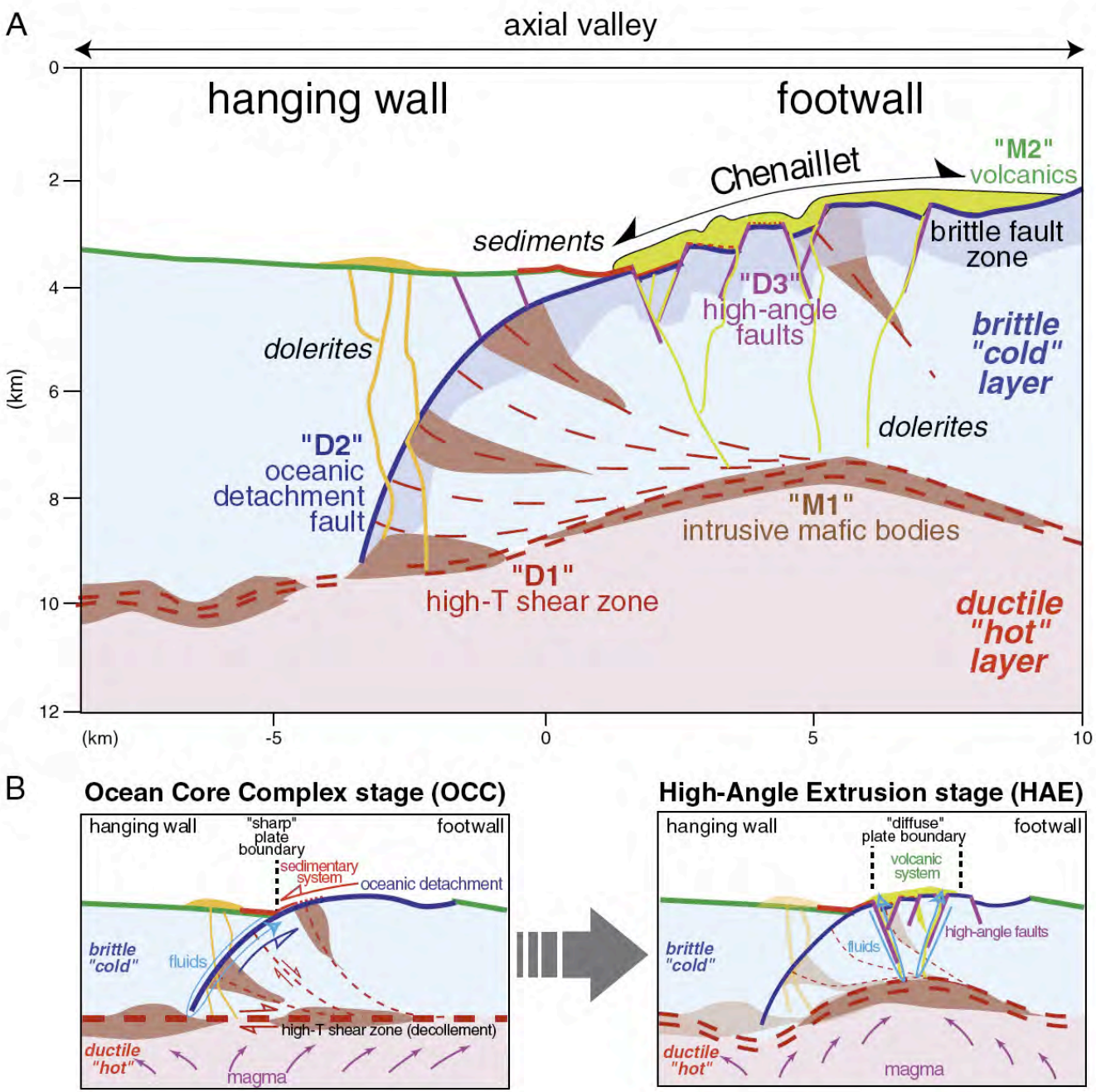

Fig. 7. (A) Model showing the final structure and contacts as observed today in the Chenaillet Ophiolite. (B) The two figures show the two stages that can be restored for the Chenaillet Ophiolite: an initial Oceanic Core Complex stage (OCC) that was overprinted by a subsequent High-Angle Extraction stage (HAE). For further explanation and discussion see text.

Manatschal et al 2011

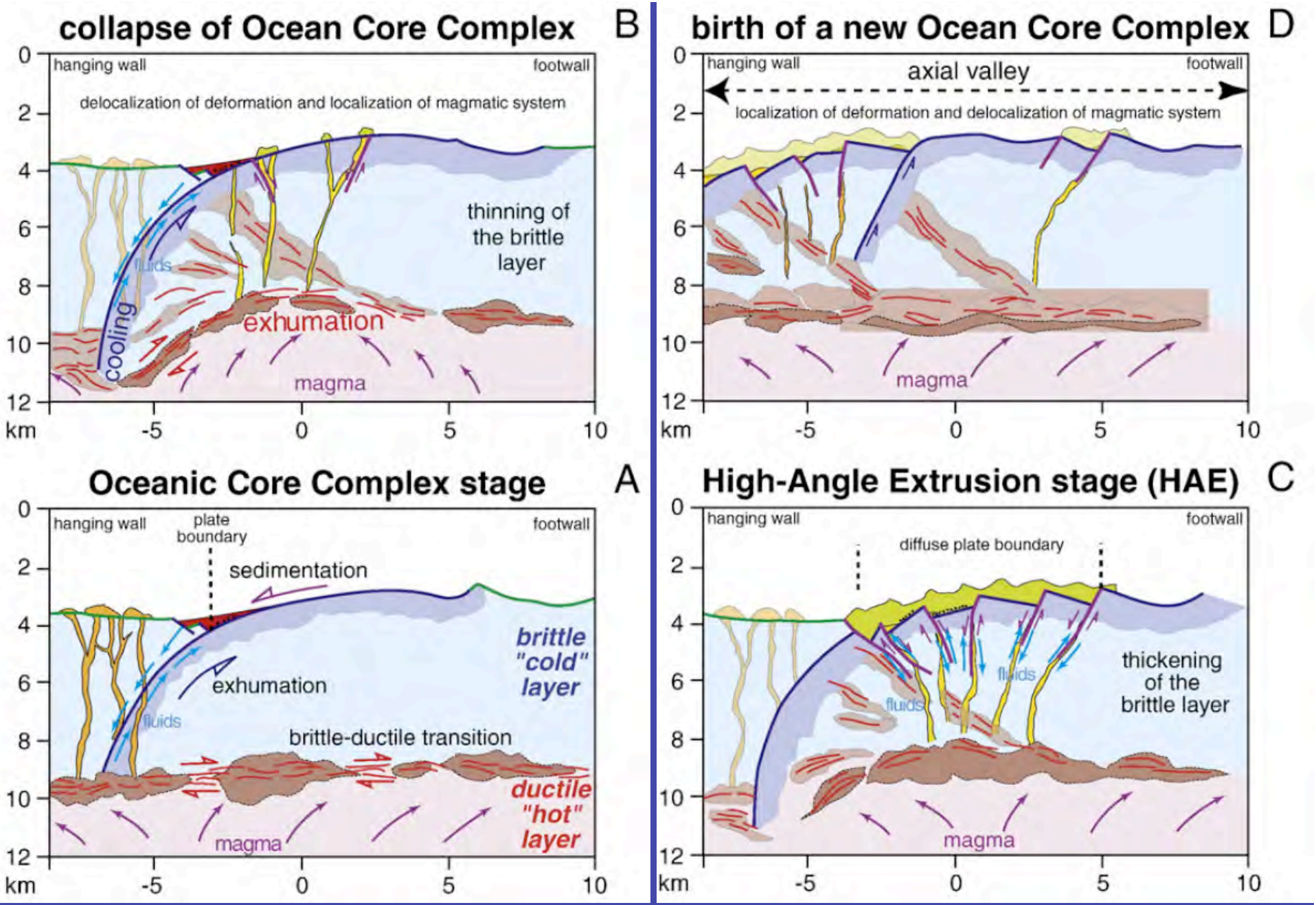

Manatschal et al 2011

Fig. 8. Conceptual model showing the life cycle of spreading structures within the axial valley of a spreading system as deduced from the observations made at the Chenaillet Ophiolite. For further discussion see text.

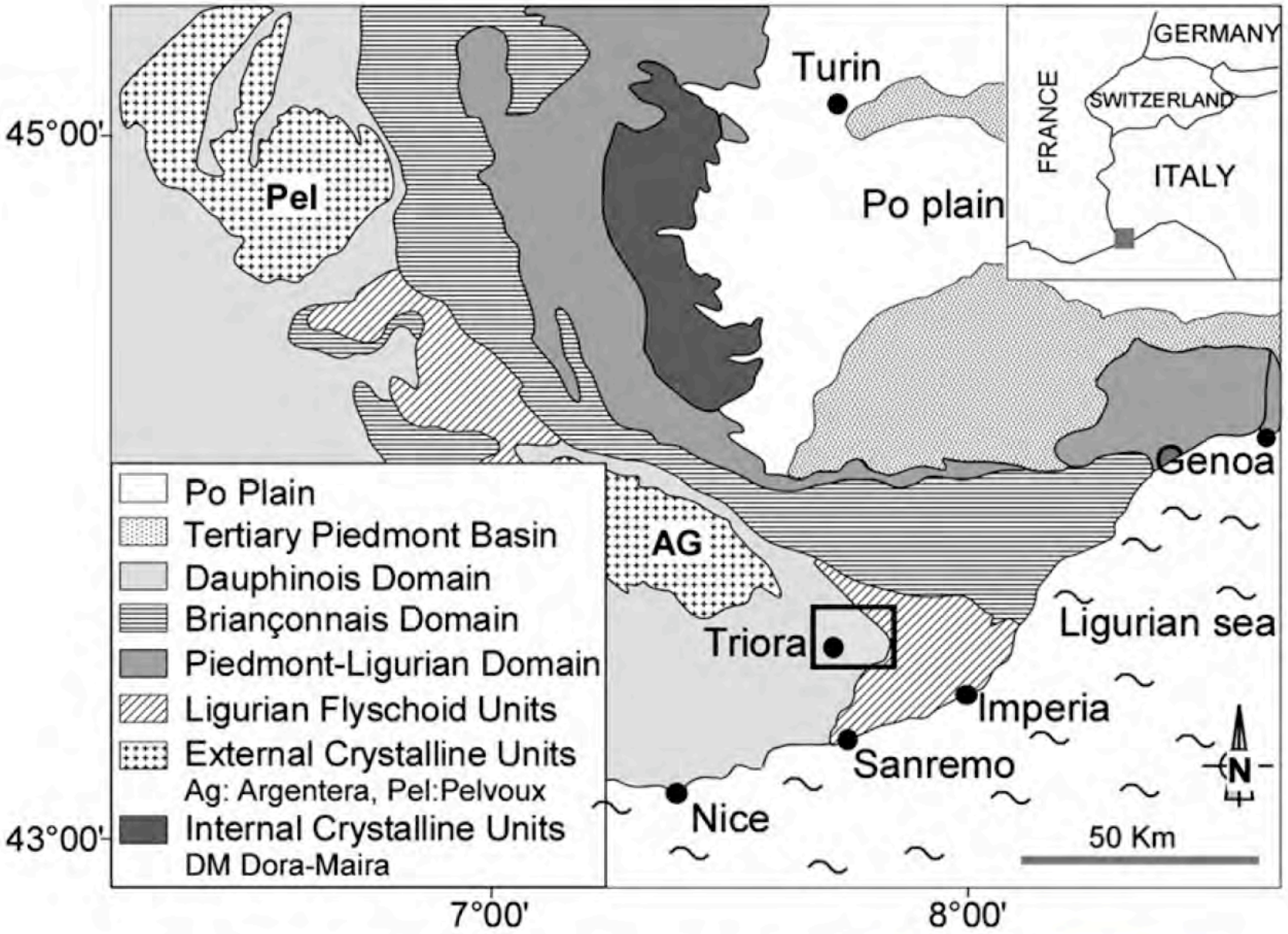

Perotti et al 2011 **Fig. 1.** Location of the study area (black square). Modified after Lanteaume (1968).

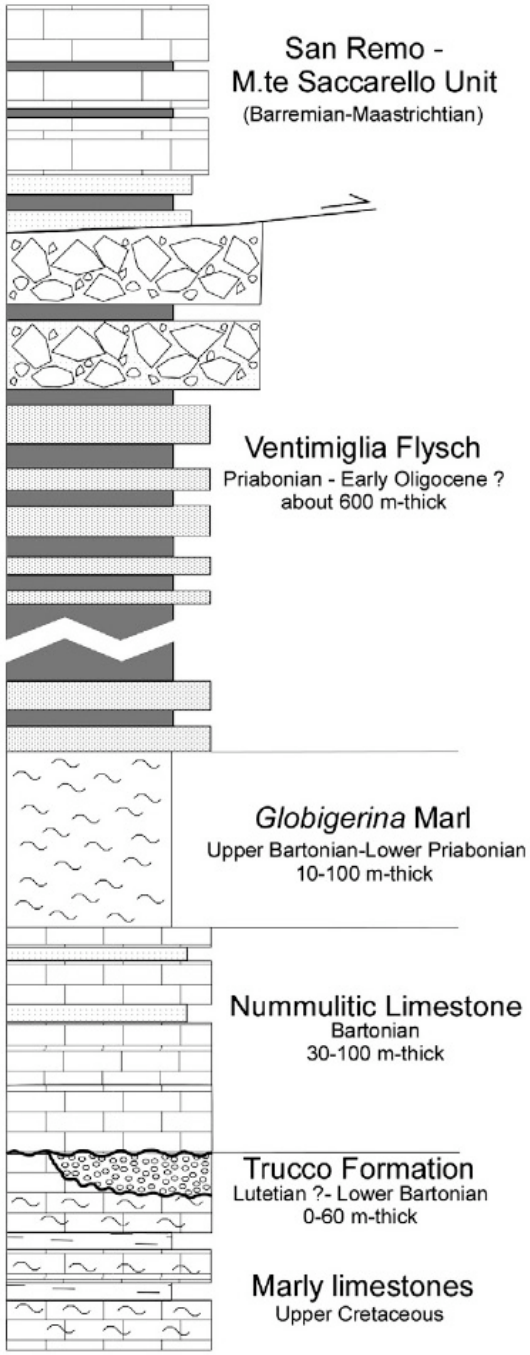

Fig. 2. Schematic log of the succession cropping out in the study area (not to scale).

Perotti et al 2011

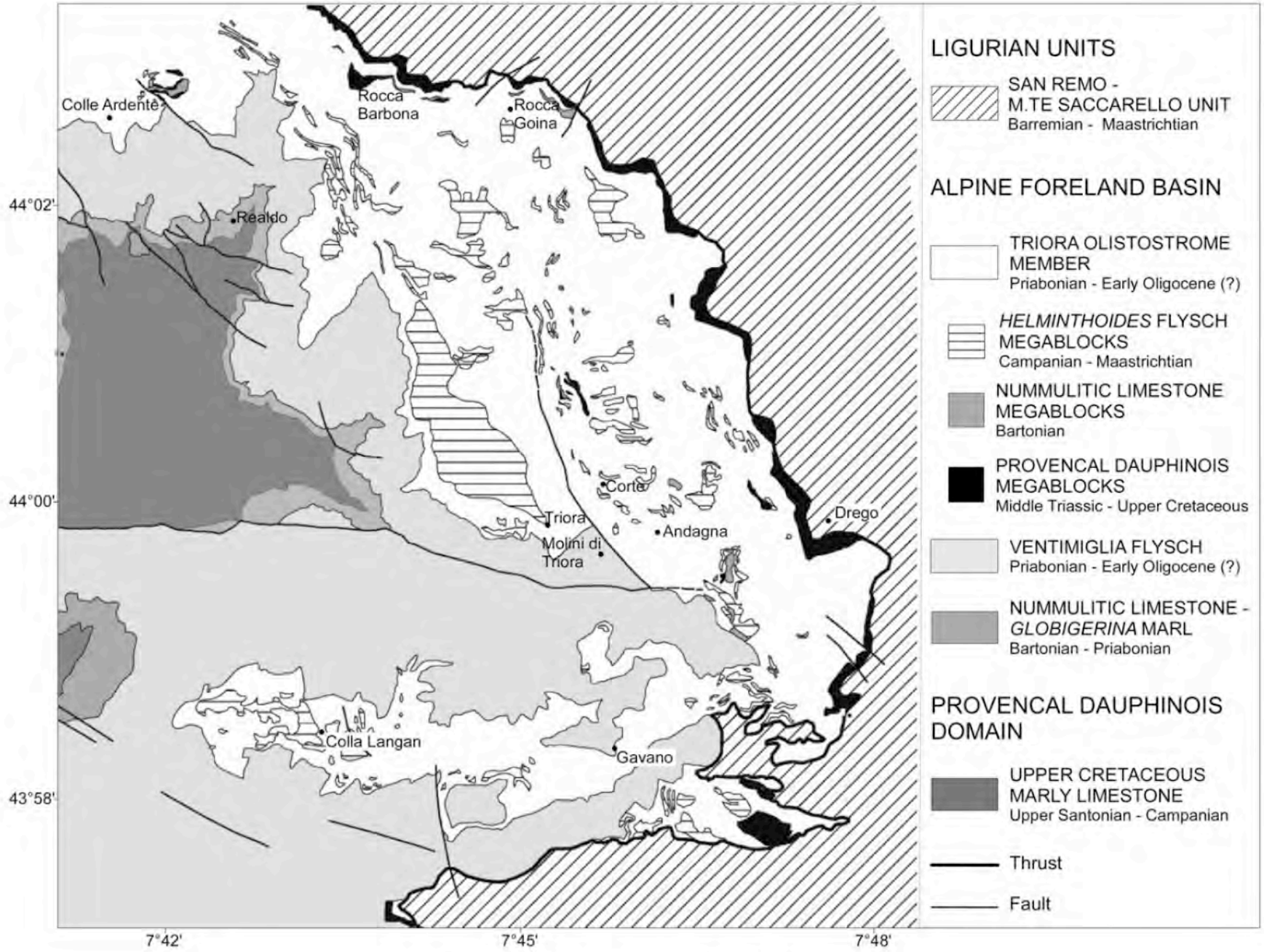

Fig. 3. Geological map of the Triora area, high Argentina valley.

Perotti et al 2011

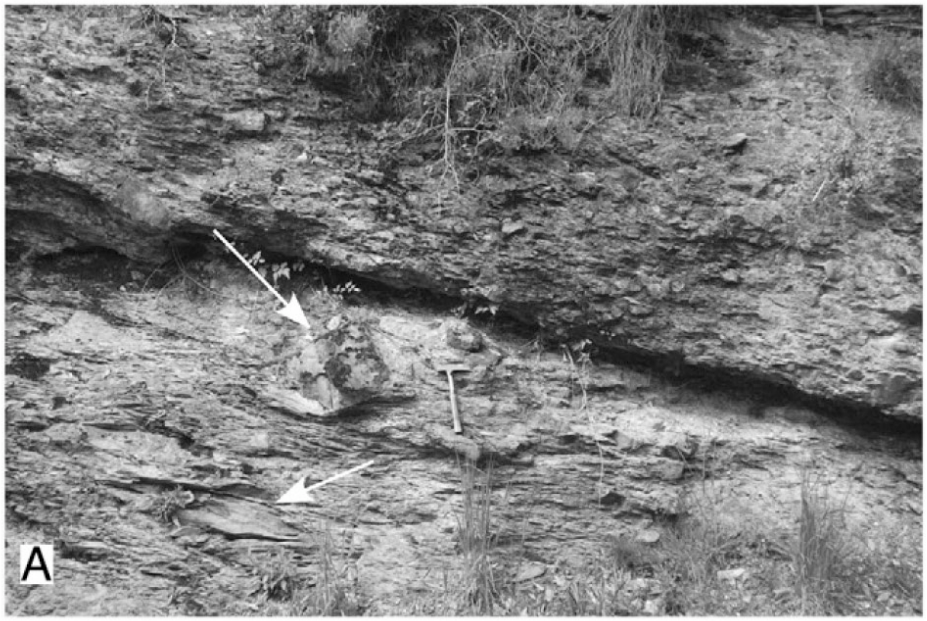

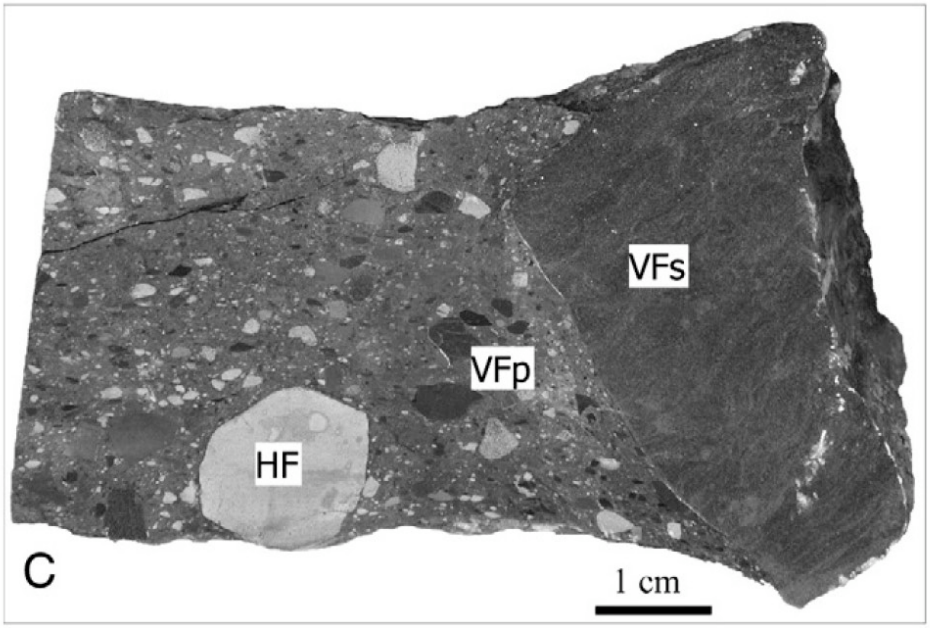

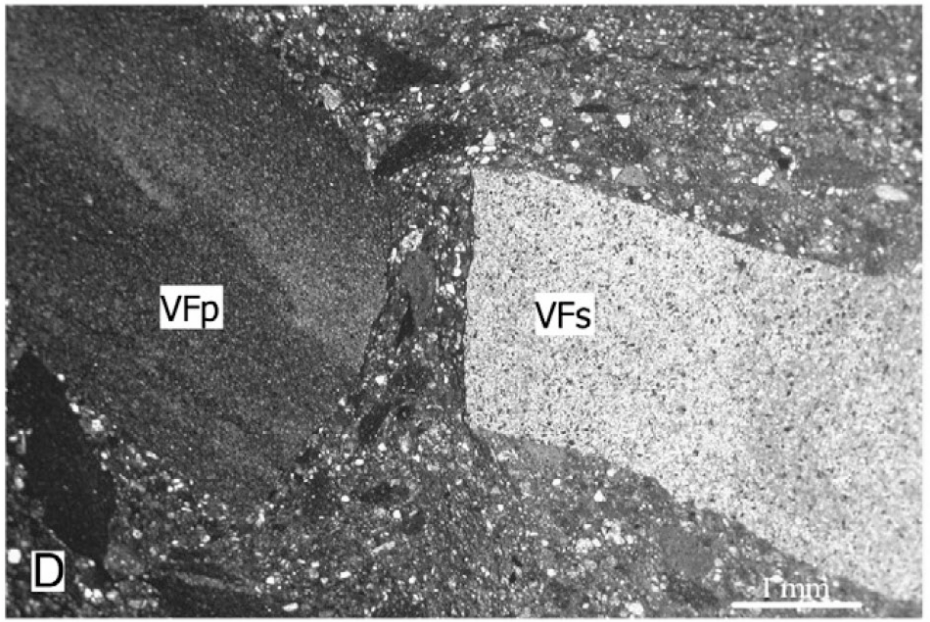

Perotti et al 2011

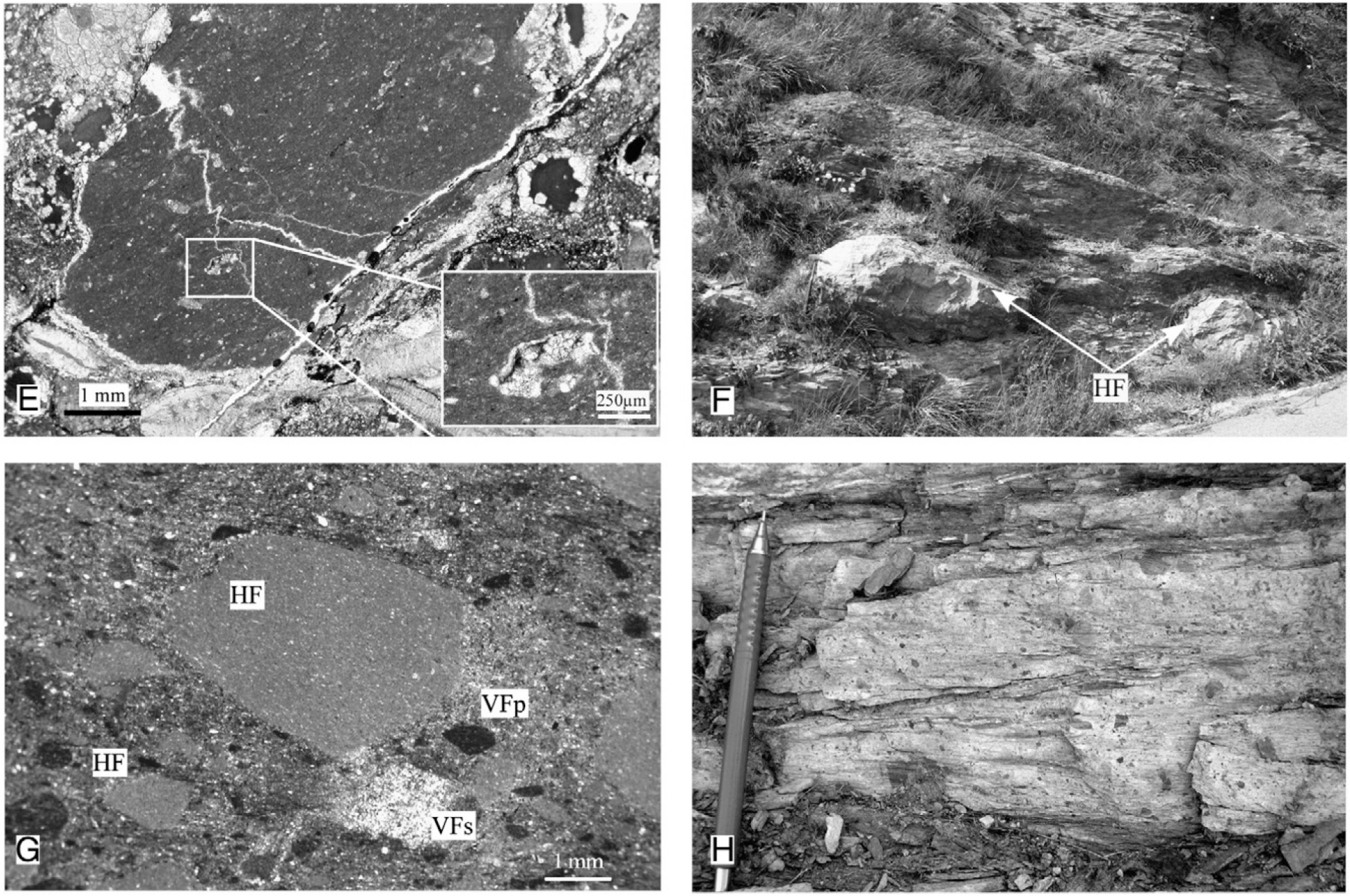

Perotti et al 2011

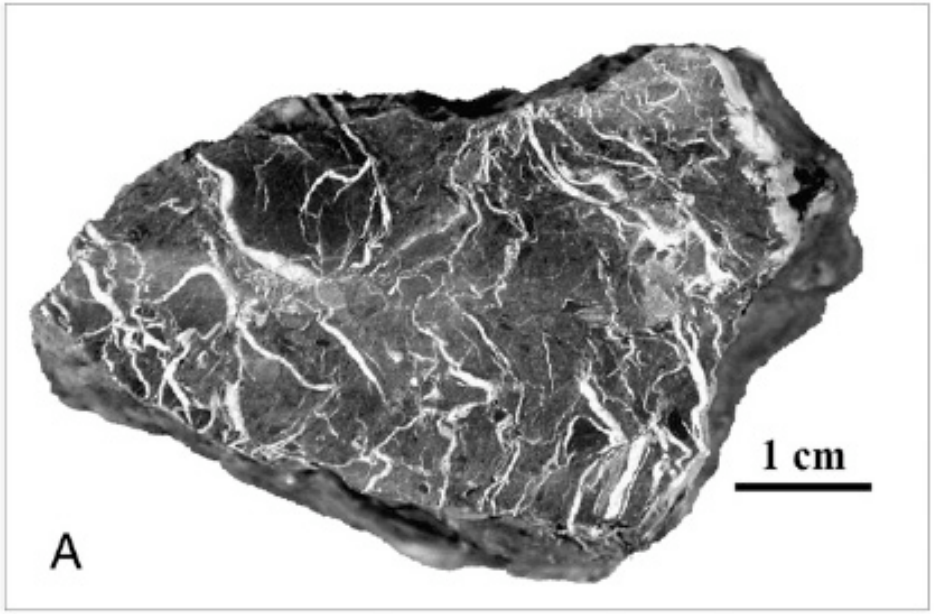

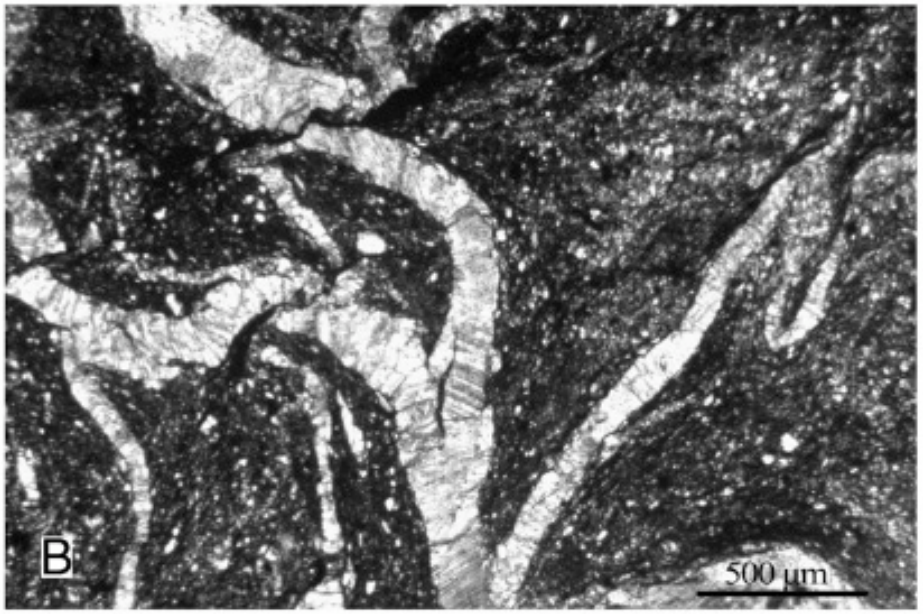

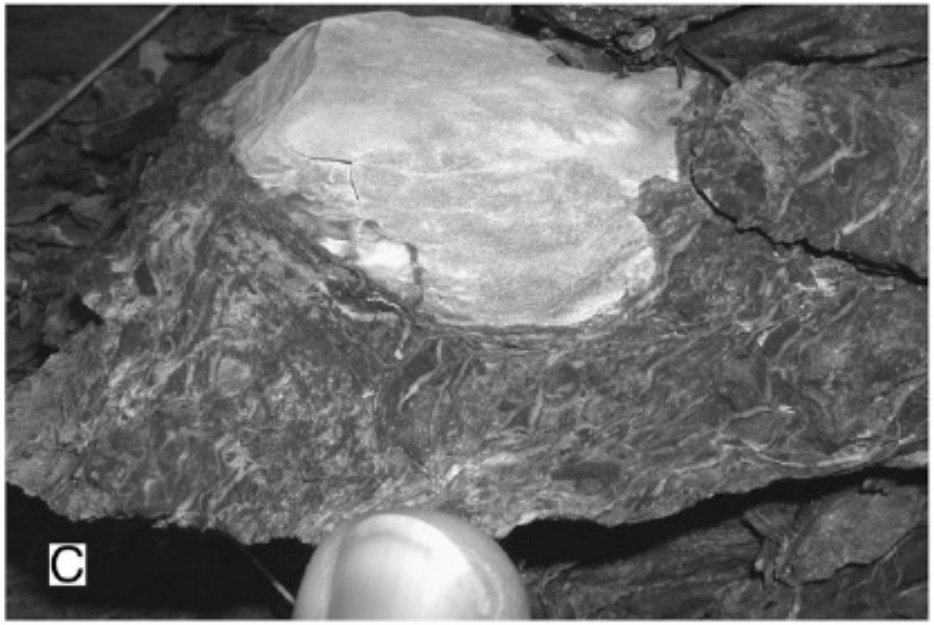

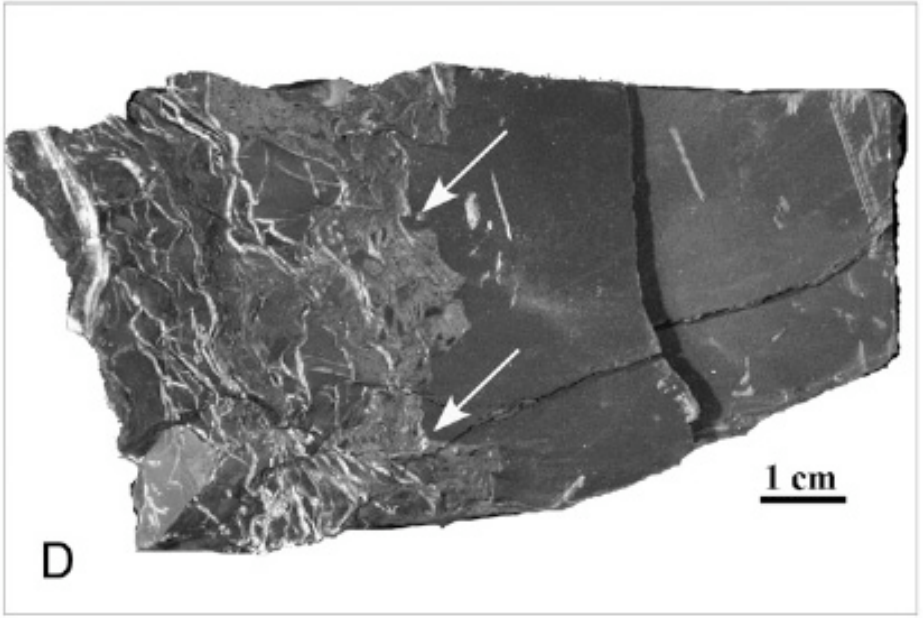

Perotti et al 201

Fig. 7. Main features of irregular calcite-filled veins crossing paraconglomerates (A, B, D, E: Andagna sector; C, F: Colleardente sector). A) Polished slab showing a dense swarm of some tens of µm-thick veins. Note the irregular and discontinuous shape of the veins. B) Photomicrograph of the veins highlighting their crumpled and broken aspect and their sparry calcite infilling. C) Paraconglomerate sample showing that veins, developed within the matrix, do not cross the clast. Finger tip for scale. D) Polished slab showing that veins are restricted into a subvertical "channel" bounded from the surrounding sediments by an irregular and sharp surface (white arrows). E, F) TL and CL photomicrographs show-

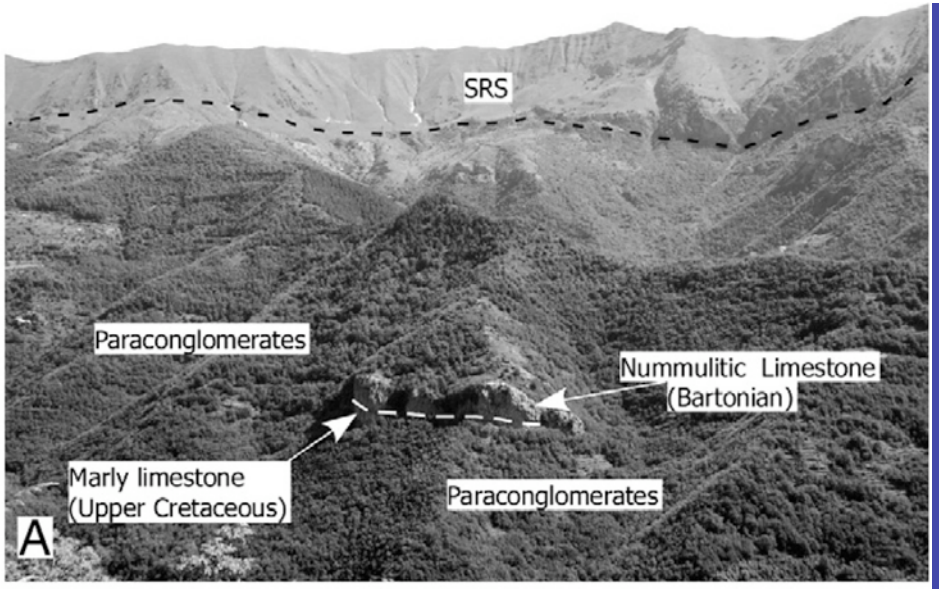

Fig. 9. Some examples of hm- to km- sized megablocks scattered in the Triora Olistostrome Member. A) Panoramic view of Corte area, showing an extraformational megablock consisting of Upper Cretaceous marly limestones overlain, with an erosional surface (hatched white line), by m-thick beds of bioclastic rudstones of Nummulitic Limestone. The megablock is embedded within paraconglomerate deposits. The hatched black line indicates the thrust at the base of the San Remo–Monte Saccarello unit (SRS). B) Panoramic view of an extraformational megablock characterized by a condensed succession ranging from Triassic dolostones to Eocene turbidites. The megablock is overlain by the thrust of the SRS unit (hatched black line), (Rocca Barbona sector). C) Km-sized, exotic megablock at Colla Langan. In the foreground, the lowermost part of the block shows a chaotic structure, characterized by disharmonic folds and bed disruption.

Perotti et al 2011

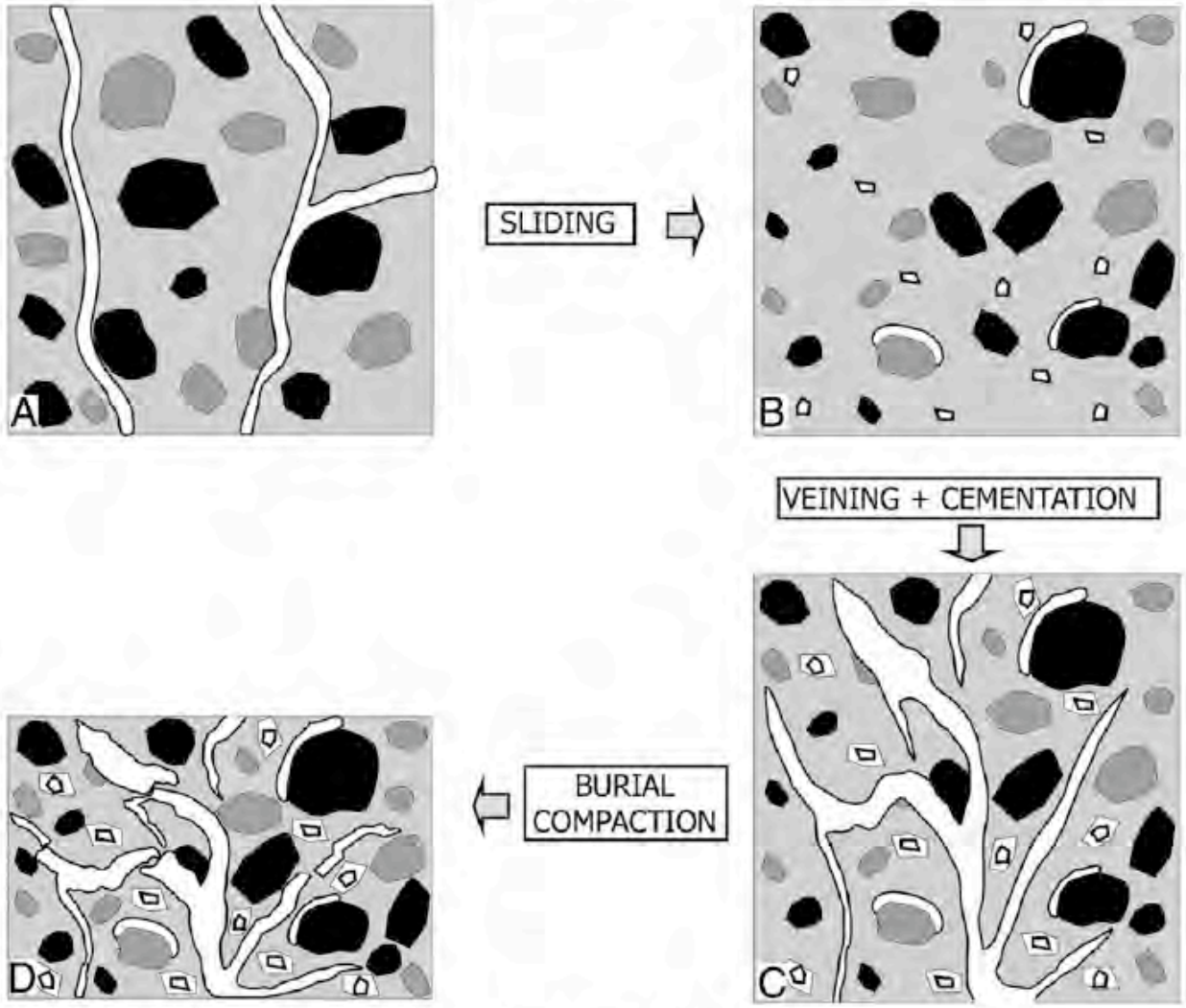

Fig. 11. Sketch synthesizing the main steps in the diagenetic evolution of paraconglomerates. A first phase of veining (A) is followed by sliding that causes production of small fragments of veins (white angular grains) and paraconglomerate clasts partly bordered by veins (B). A second phase of veining takes place and is associated with calcite overgrowth around vein fragments (C). Finally, burial compaction produces breakage and crumpling of the second vein generation (D).

Perotti et al 2011

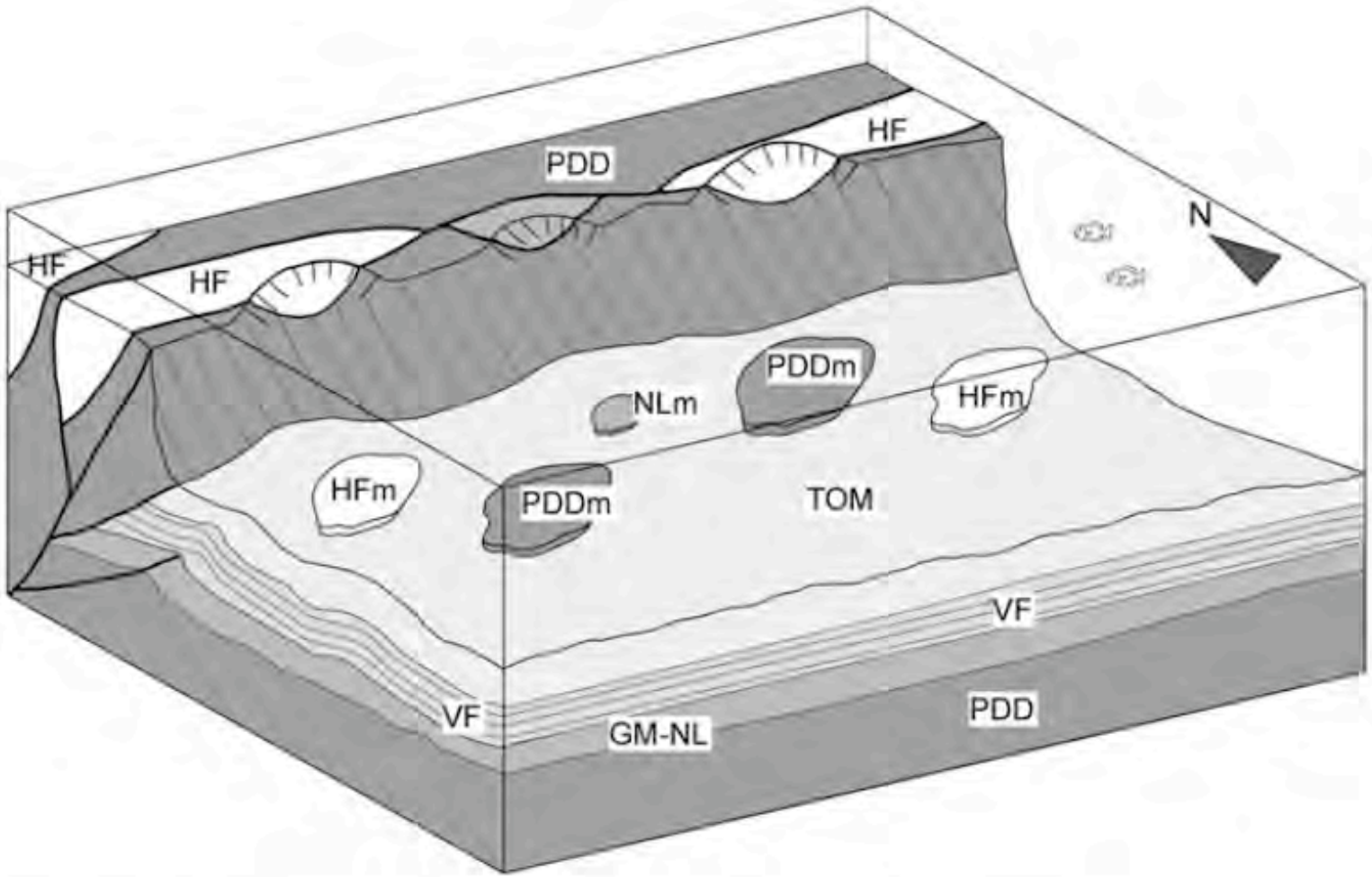

Fig. 12. Block diagram depicting the geotectonic setting in which TOM was formed. For further details see text. HF: *Helminthoides* Flysch; HFm: *Helminthoides* Flysch megablock; GM–NL: *Globigerina* Marls–Nummulitic Limestone; NLm: Nummulitic Limestone megablock; PDD: Provençal Dauphinois Domain; PDDm: Provençal Dauphinois Domain megablock; TOM: Triora Olistostrome member; VF: Ventimiglia Flysch. Orientation of the diagram is purely indicative and refers to present-day coordinates.

Perotti et al 201

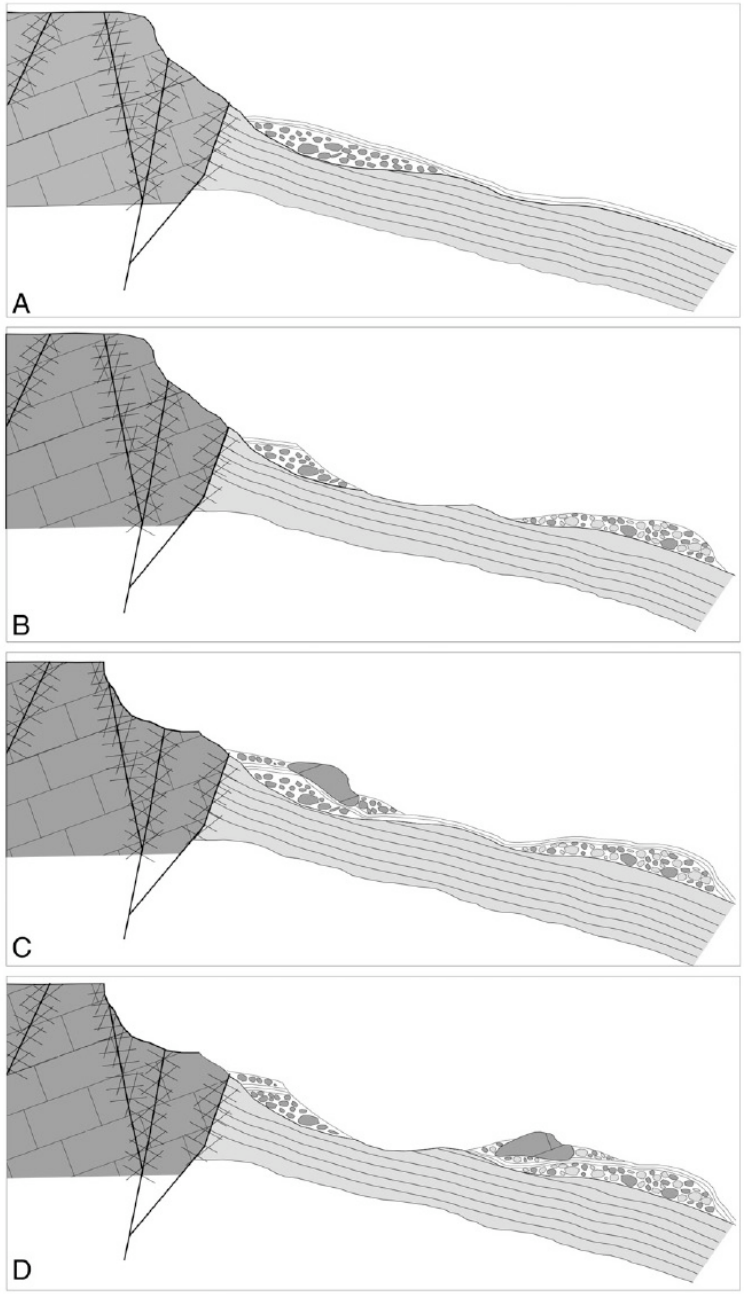

Fig. 13. Schematic sketch summarizing the main steps in the genesis of the TOM. Clasts of lithified carbonate units, exposed in fault-bounded, internally fractured, ridges, accumulate as breccias at the foot of the scarp and are covered by fine grained turbidites (A). Slope failures involve breccias and turbidite deposits including concretions and disrupted cemented beds giving rise to polygenic paraconglomerates (B). Catastrophic rock falls generate emplacement of megablocks (C) that may be further involved in gravitational movements together with breccias and paraconglomerates (D).

Perotti et al 2011

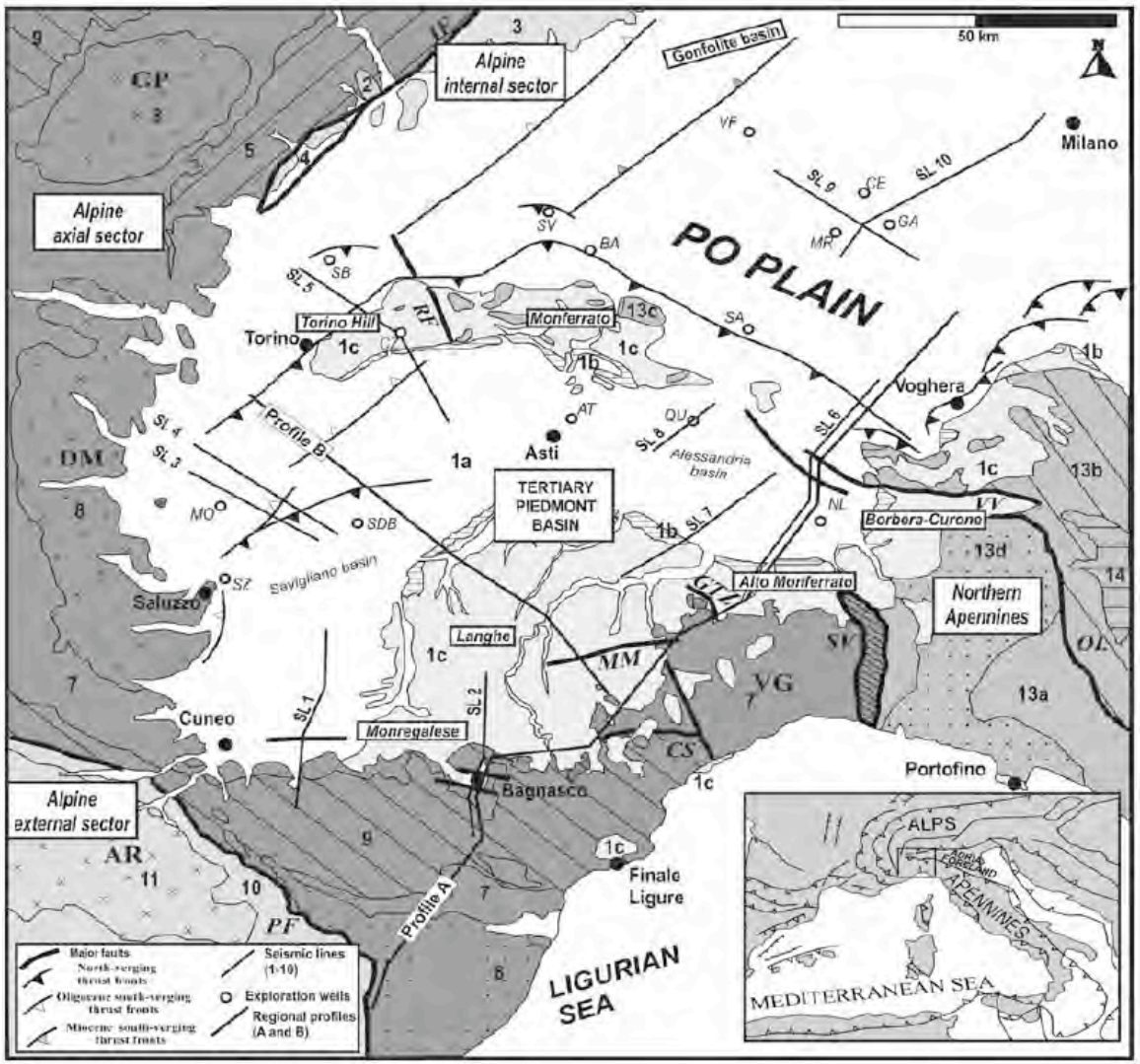

Fig. 1 Geological sketch map of the investigated Alps—Apennines junction area (modified after C.N.R. 1983). Syn- to post-orogenic rocks—(*1a*) Pliocene to Holocene, (*1a*) Messinian, (*1a*) Upper Eocene to Tortonian. (*2*) Periadriatic Tertiary intrusives. Alpine internal sector—(*3*) Southern Alpine units, (*4*) Canavese basement and cover units. Alpine axial sector—(*5*) Sesia Zone, (*6*) Helmintoid flysch units, (*7*) Piedmont- Ligurian ophiolite bearing nappes, (*8*) Internal Crystalline Massifs, (*9*) Gran San Bernardo nappe and relative Briançonnais sedimentary cover. Alpine external sector—(*10*) Dauphinois-Helvetic cover units, (*11*) Late-Hercynian deposits and basament units of the External Crystalline Massifs, Northern Apennines—(*13*) Ligurian units: (*a*) internal Ligurides, (*b*) external Ligurides, (*c*) Ligurian and chaotic complexes of Monferrato, (*d*) Antola unit, (*14*) Upper Eocene-Lower Miocene sub-Ligurian and Tuscan units (Bobbio window). Major faults. *CS* Celle-Sanda, *GTZ* Grognardo Thrust Zone, *IF* Insubric Fault, *MM* Merana-M.Acuto, *OL* Ottone-Levanto, *PF* Frontal Pennine Fault, *RF* Rio Freddo, *SV* Sestri Voltaggio, *VV* Villavernia-Varzi. Acronyms: *AR* Argentera, *DM* Dora Maira, *GP* Gran Paradiso, *VA* Valosio, *VG* Voltri Group. Traces of the buried thrusts are modified after C.N.R. (1983) on the basis of the present work. Exploration wells: *AT* Asti, *BA* Balzola, *CE* Cerano, *CZ* Cinzano, *GA* Garlasco, *MO* Moretta, *MR* Mortara, *NL* Novi Ligure, *QU* Quargnento, *SA* Sartirana, *SB* San Benigno, *SDB* Sommariva del Bosco, *SV* Sali Vercellese, *SZ* Saluzzo, *VF* Villafortuna

Mosca et al 2009

Fig. 2 Stratigraphic framework (comprehensive of both outcrop and subsurface data) of the Upper Eocene to Miocene deposits overlying the tectonic junction between Alps and Northern Apennines (modified after Mosca 2006 and Rossi et al. 2009). Inset shows approximately the area covered by the scheme. *White triangles* shallowing-upward, *gray triangles* deepening-upward. Unconformities (from *bottom* to *top*): *B-PR* base Priabonian, *B-RU* base Rupelian, *I-RU* intra-Rupelian, *L-RU* Late Rupelian, *B-CH* base Chattian, *L-CH* latest Chattian, *I-BU* intra-Burdigalian, *L-BU* Late Burdigalian, *B-LA* base Langhian, *B-SE* base Serravallian, *L-SE* latest Serravallian, *L-TO* Late Tortonian, *I-ME* intra-Messinian, *L-ME* Late Messinian. Basins in the text: *MR* Molare-Rocchetta, *SR* Savignone-Ranzano

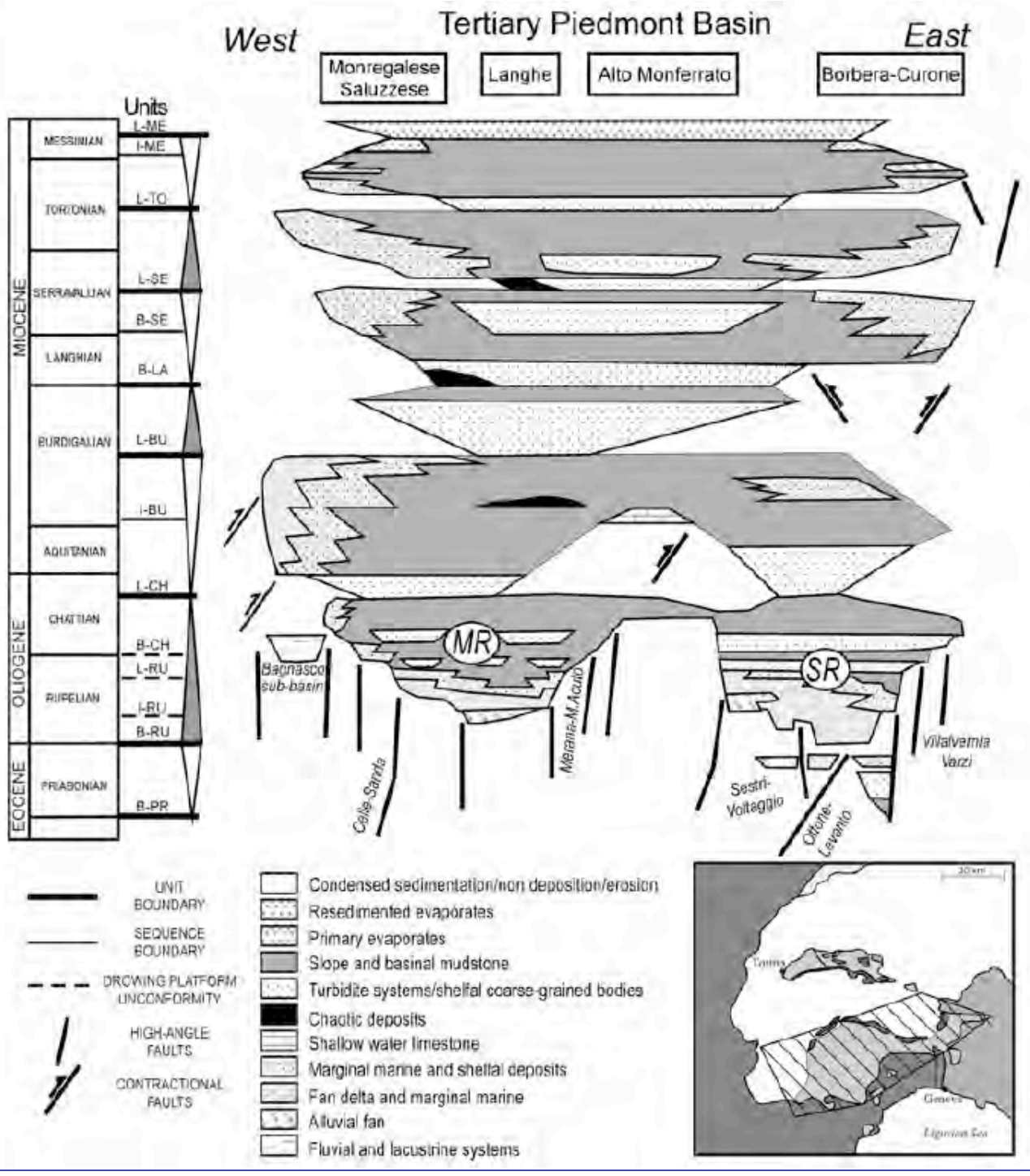

Mosca et al 2009

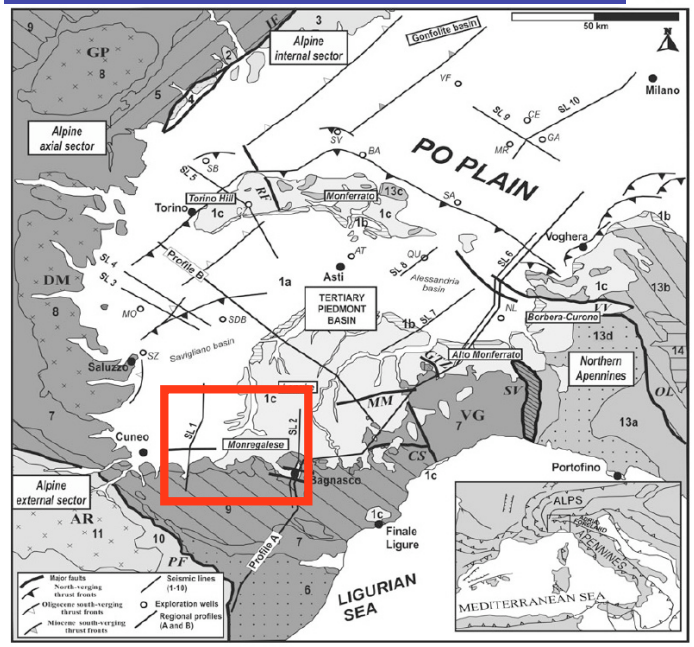

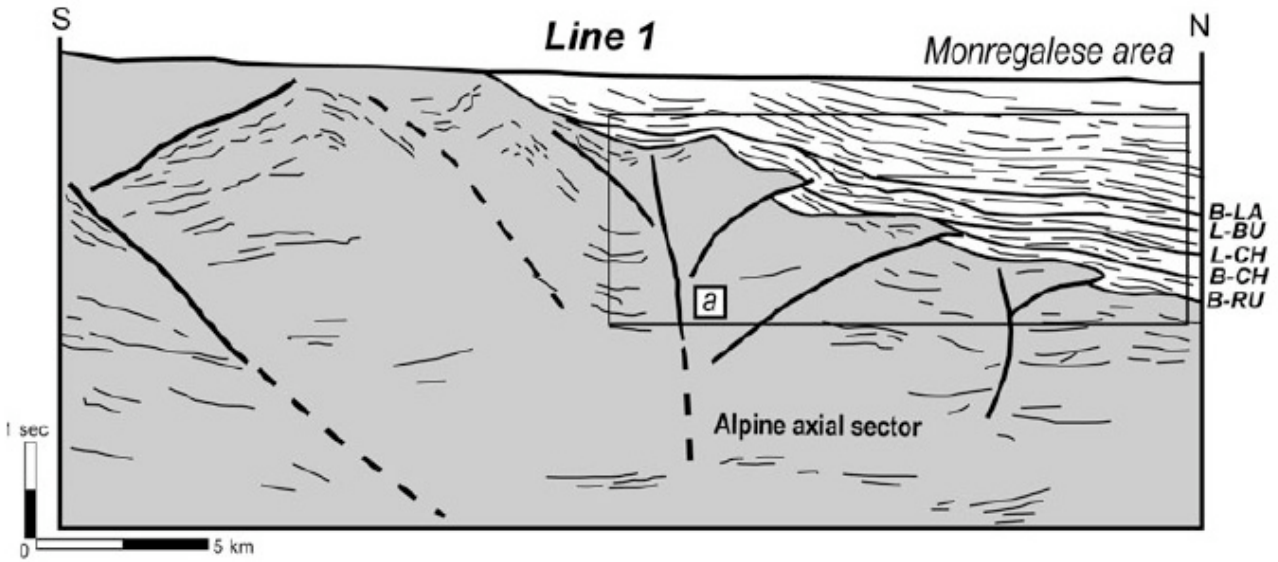

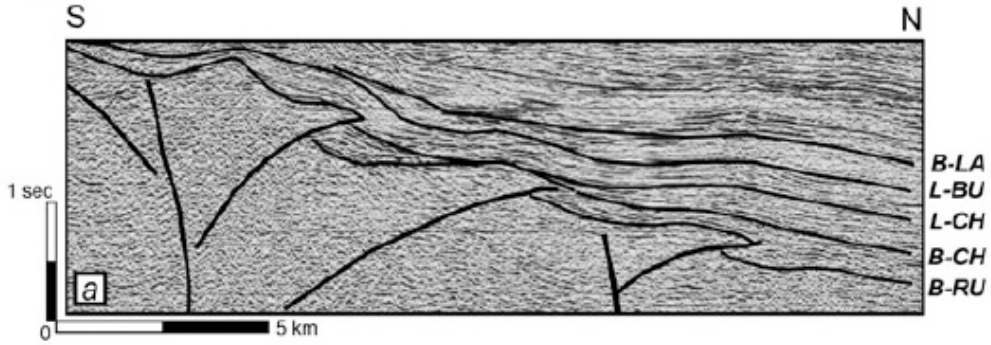

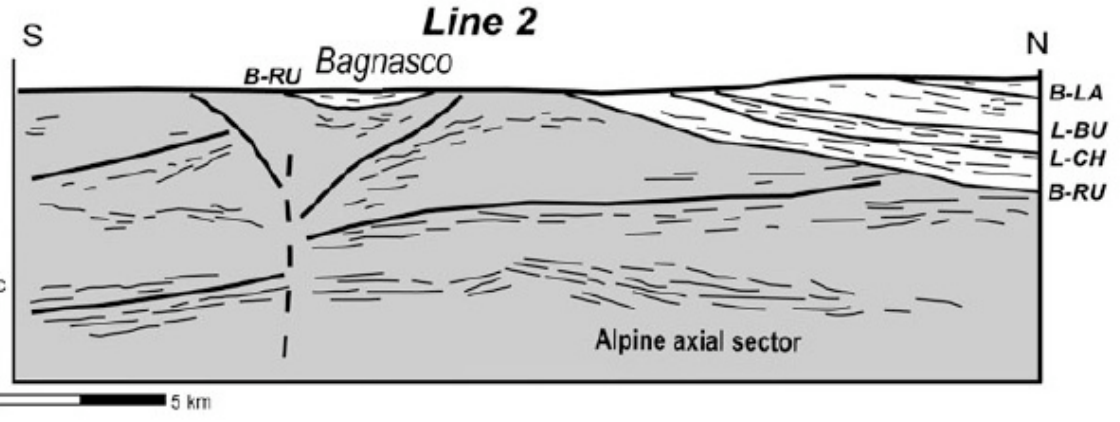

Mosca et al 2009

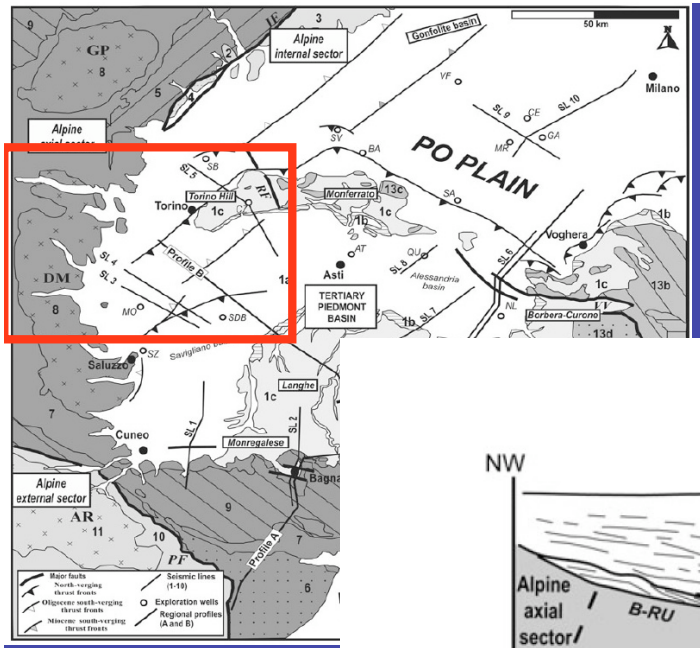

Line 3

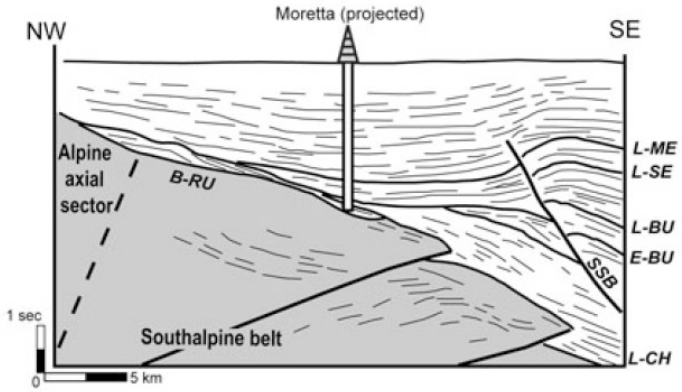

Line 4

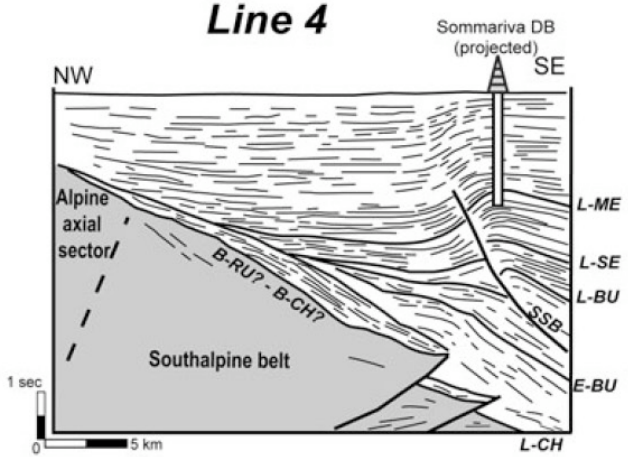

Line 5

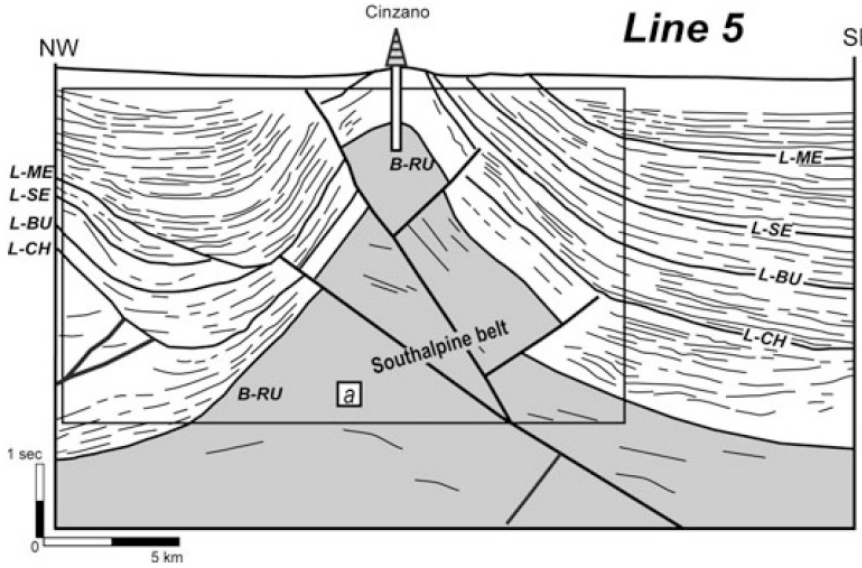

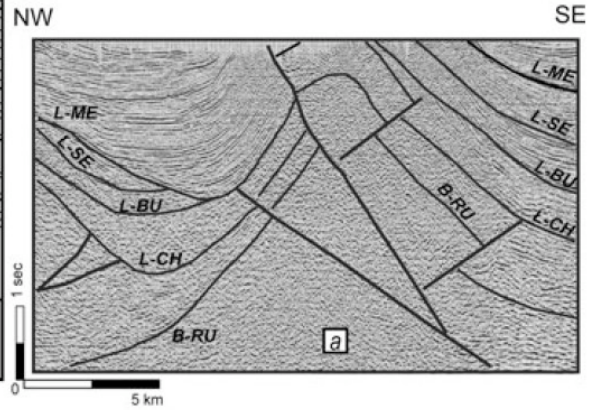

Mosca et al 2009

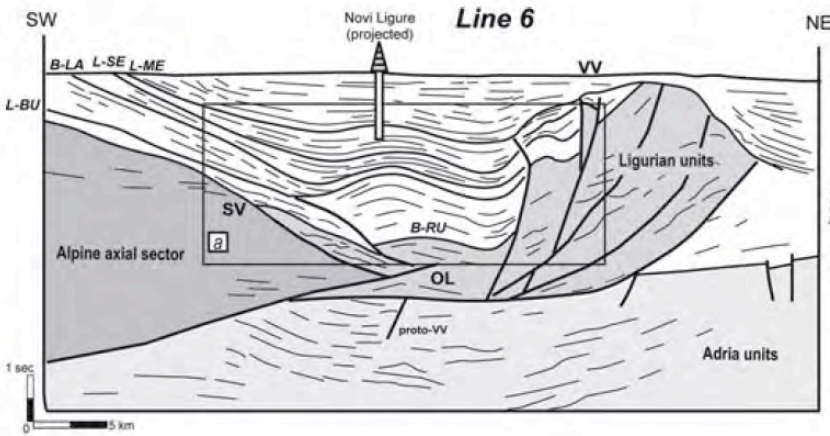

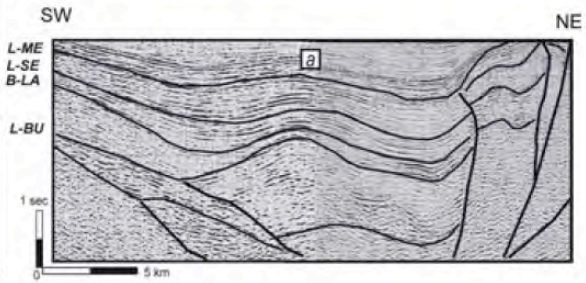

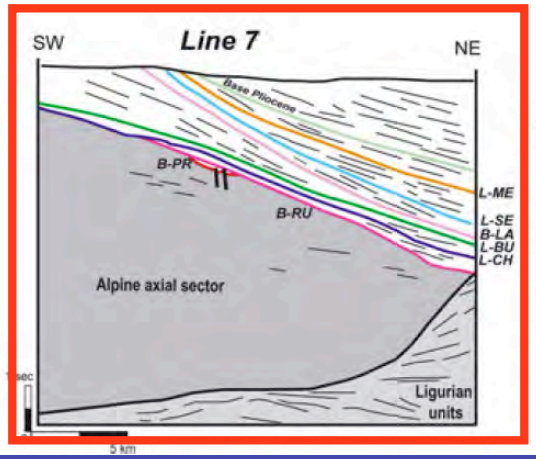

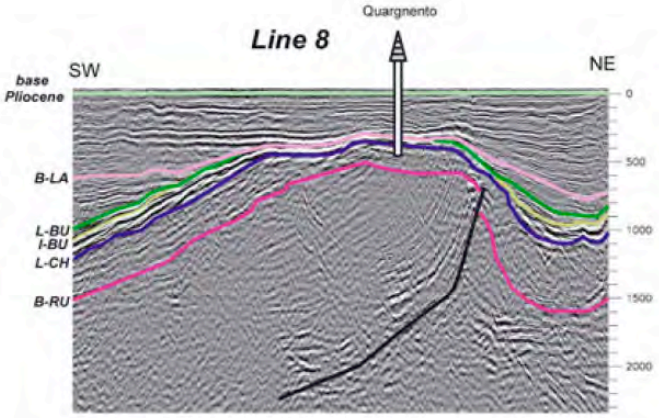

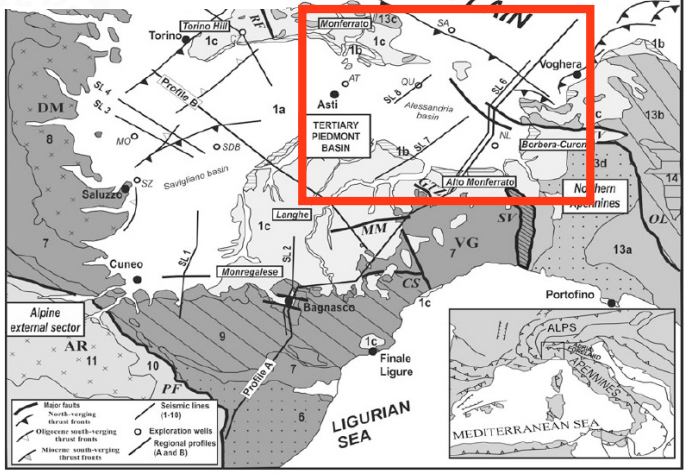

Mosca et al
2009

Fig. 8 Tectono-sedimentary evolution of the Alto Monferrato sector and its lateral buried continuation defined through three successive flattenings along part of seismic line 7. Horizontal Datum Planes: infra-Burdigalian (time 1), top Burdigalian (time 2) and top Messinian (time 3). The unconformity codes are in Fig. 2

Time 1: infra-Burdigalian

Time 2: top Burdigalian

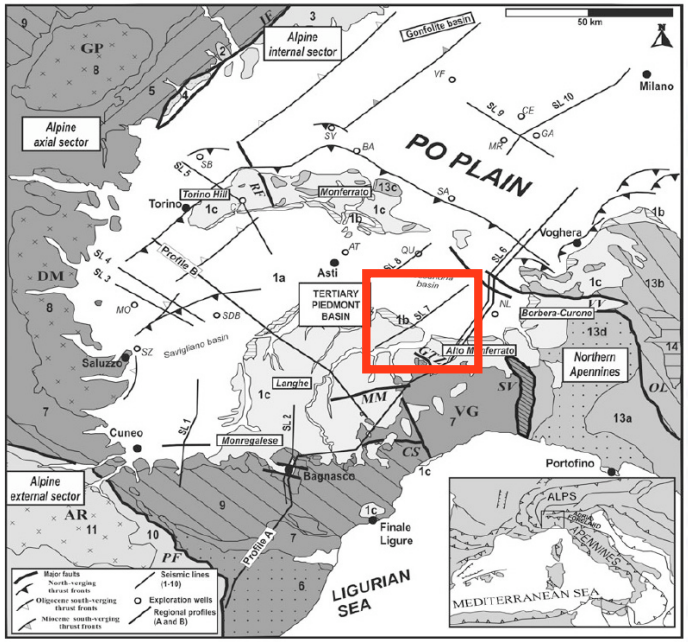

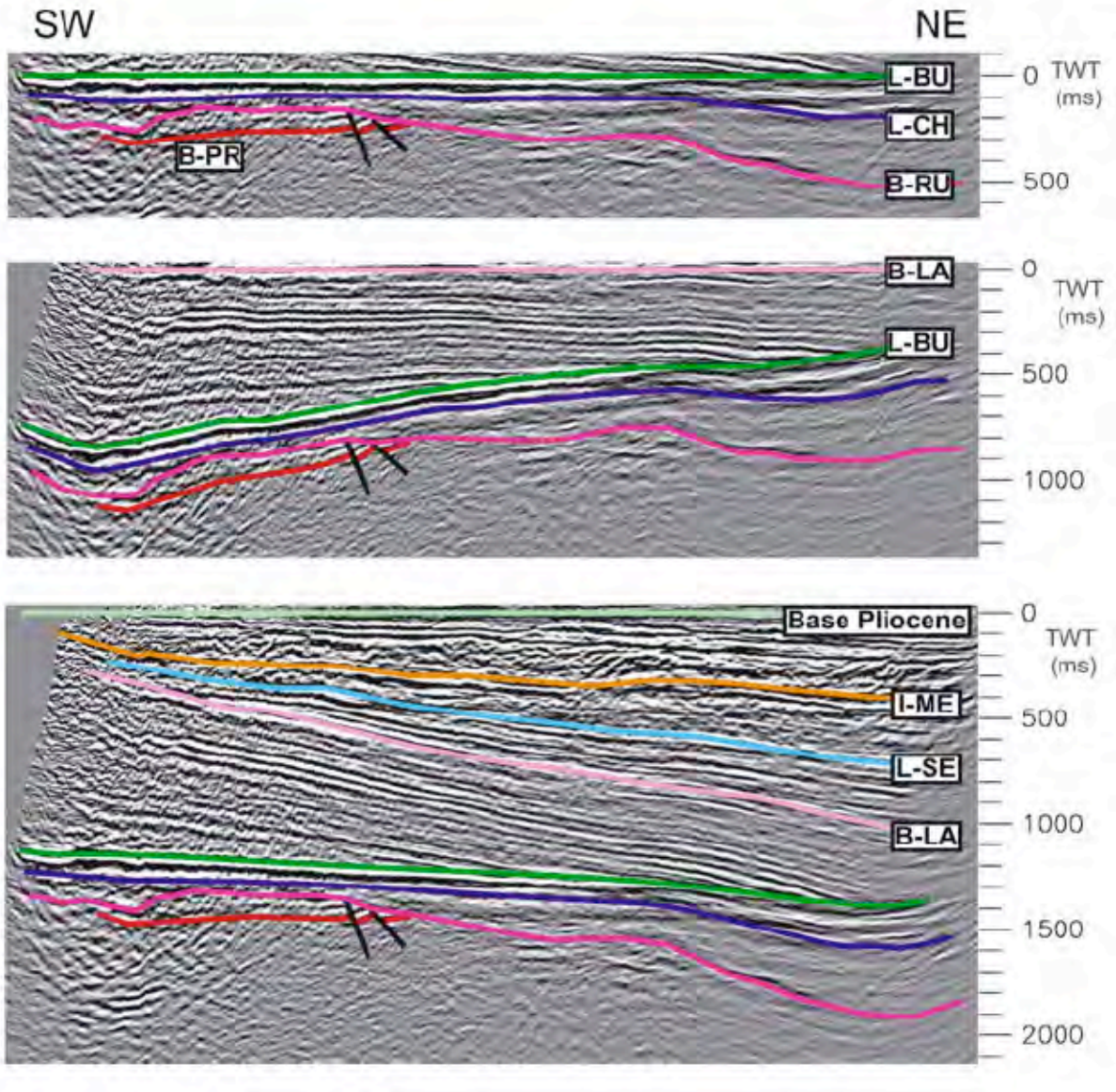

Mosca et al 2009

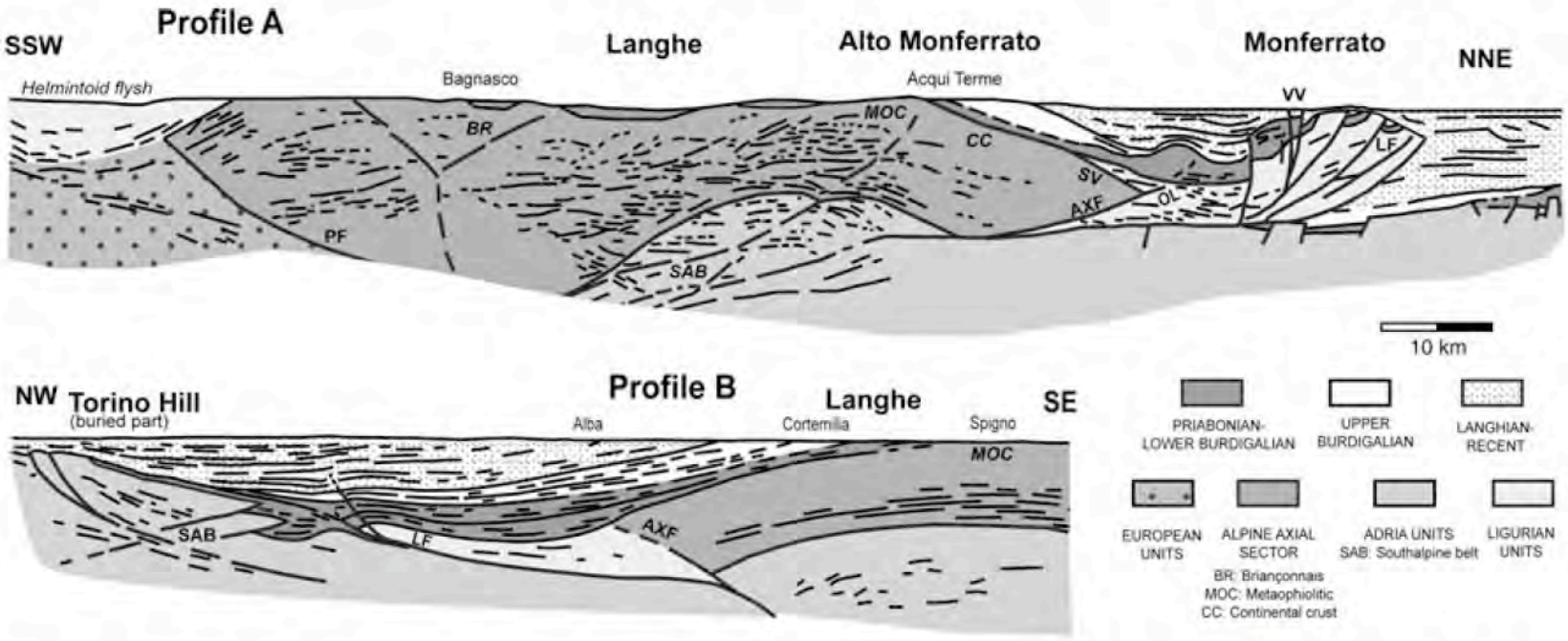

Fig. 10 Regional geological profiles across the Alps–Apennines junction area. Trace of profiles are in Fig. 1 (*AXF* Front of the Alpine axial sector, *LF* Ligurian Fronts, *OL* Ottone-Levanto, *PF* Penninic Front, *SV* Sestri-Voltaggio, *VV* Villavernia-Varzi)

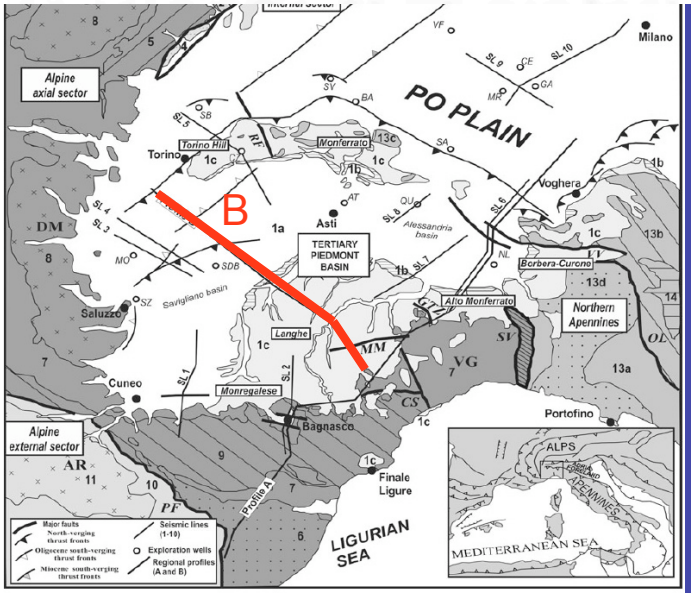

Mosca et al 2009

Fig 11 Profile showing the tectonic control on basin development and architecture. The unconformity codes are in Fig. 2

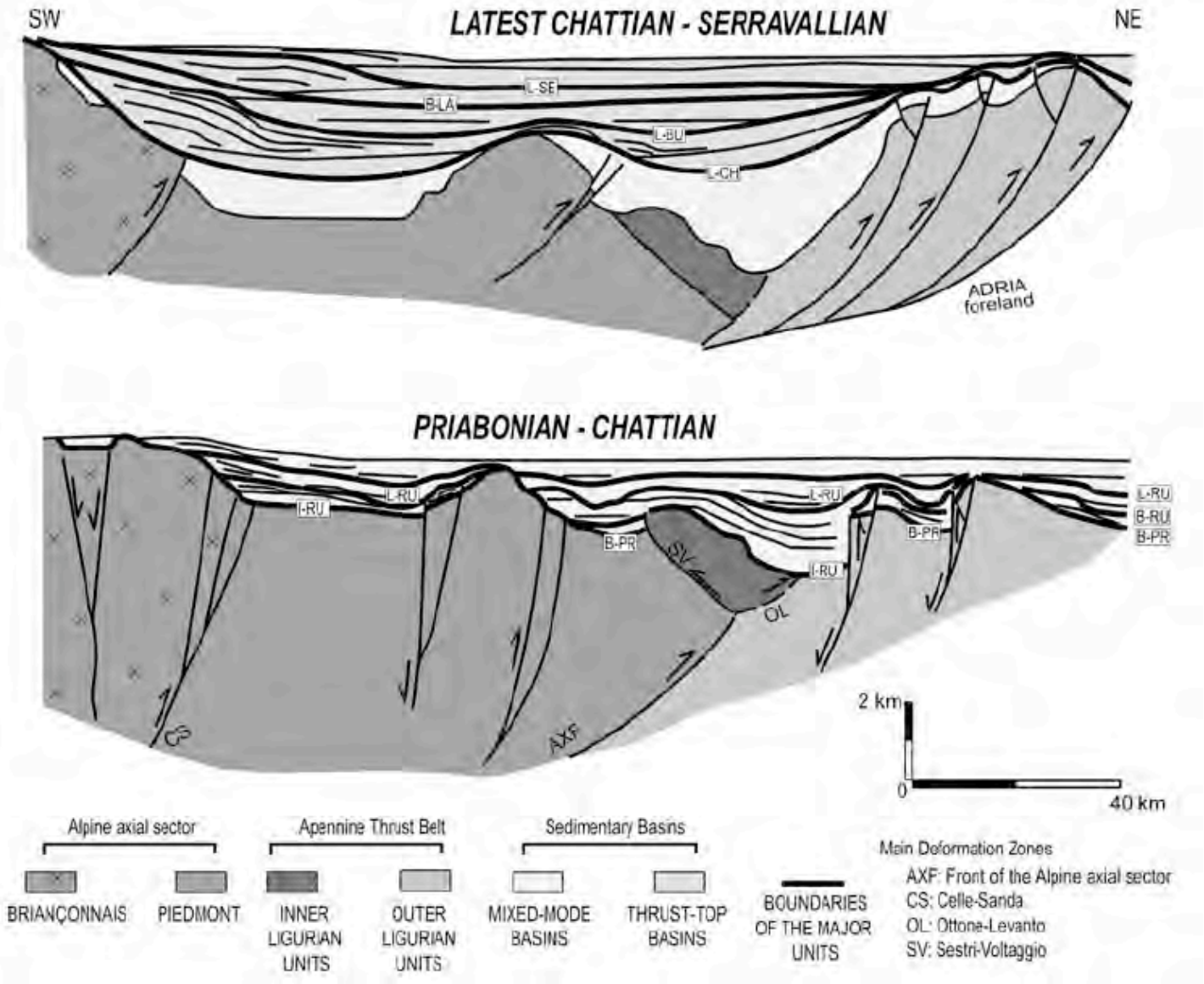

Mosca et al 2009

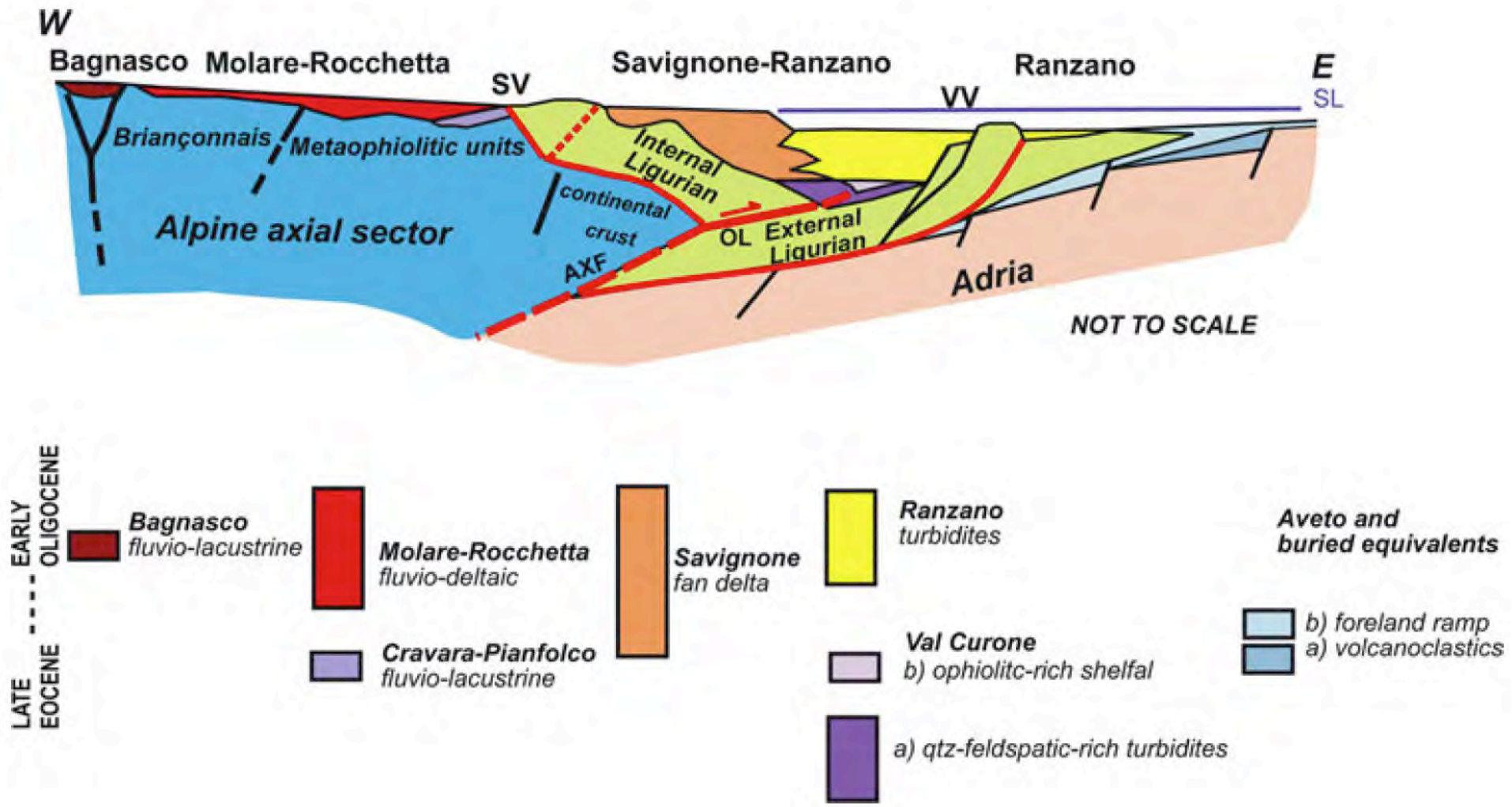

Mosca et al 2009

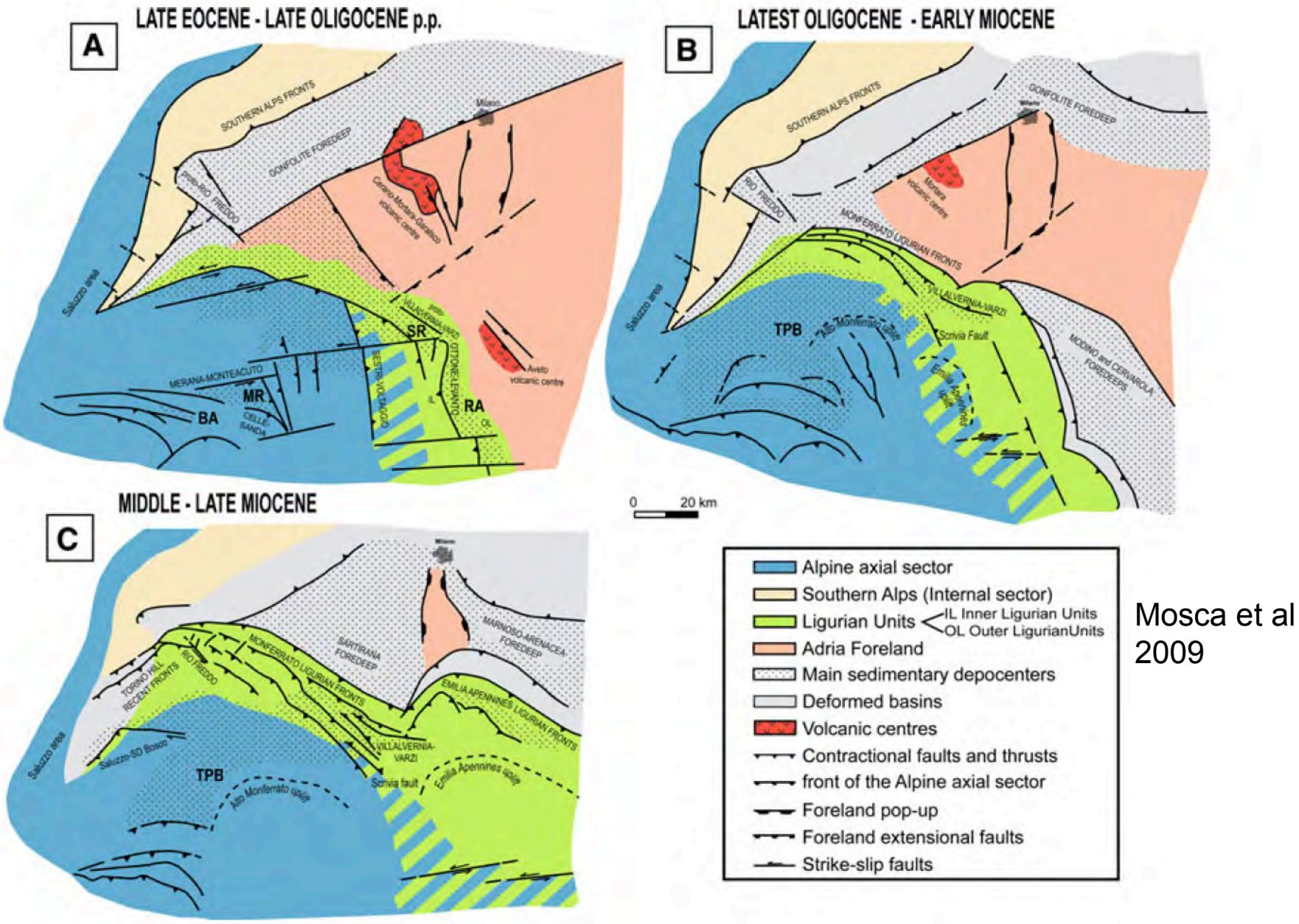

Mosca et al 2009

Fig. 9 Paleotectonic maps illustrating the Late Eocene to Miocene evolution of the Alps–Apennines junction (see discussion in the text). The codes for the basins are: *BA* Bagnasco, *MR* Molare-Rocchetta, *RA* Ranzano, *SR* Savignone-Ranzano, *TPB* Tertiary Piedmont Basin